CLASSIFICATION: BIOLOGICAL SCIENCES: Evolution

TITLE: Genomics of sorghum local adaptation to a parasitic plant

AUTHORS: Emily S. Bellis[1], Victoria L. DeLeo[1], Elizabeth A. Kelly[1], Claire M. Lorts[1], Germinal Rouhan[2], Andrew Budden[3], Govinal Badiger Bhaskara[4], Zhenbin Hu[5], Robert Muscarella[6], Thomas E. Juenger[4], Michael P. Timko[7], Geoffrey P. Morris[5], Claude W. dePamphilis[1], Jesse R. Lasky[1]

[1]Department of Biology, Pennsylvania State University, University Park, PA, 16802
[2]Institut Systématique Evolution Biodiversité (ISYEB), Muséum national d'Histoire naturelle, CNRS, Sorbonne Université, EPHE, 57 rue Cuvier, CP39, 75005 Paris, France
[3]Royal Botanic Gardens, Kew, Richmond TW9 3AB, UK
[4]Department of Integrative Biology, 2415 Speedway #C0930, University of Texas, Austin, TX, 78712
[5]Department of Agronomy, Kansas State University, Manhattan, Kansas, 66506
[6]Department of Plant Ecology and Evolution, Evolutionary Biology Centre, Uppsala University, SE-75236 Uppsala, Sweden
[7]Department of Biology, University of Virginia, Charlottesville, Virginia, 22904

CORRESPONDING AUTHOR: Emily S. Bellis, Department of Biology, Pennsylvania State University, University Park, PA, 16802, ezb336@psu.edu

ABSTRACT:

Host-parasite coevolution can maintain high levels of genetic diversity in traits involved in species interactions. In many systems, host traits exploited by parasites are constrained by use in other functions, leading to complex selective pressures across space and time. Here, we study genome-wide variation in the staple crop *Sorghum bicolor* (L.) Moench and its association with the parasitic weed *Striga hermonthica* (Delile) Benth., a major constraint to food security in many African countries. We hypothesize that sorghum landraces are subject to geographic selection mosaics within parasite-prone areas and selection against resistance where *S. hermonthica* is never found. Supporting this hypothesis, multiple independent loss-of-function alleles at sorghum *LOW GERMINATION STIMULANT 1* (*LGS1),* a locus known to impact resistance, are broadly distributed among African landraces and geographically associated with *S. hermonthica* occurrence, suggesting a role in local adaptation to parasite pressure. However, the low frequency of these alleles within *S. hermonthica*-prone regions and their absence elsewhere indicates potential trade-offs restricting their distribution. *LGS1* impacts stereochemistry of strigolactones, hormones controlling plant architecture, belowground signaling with other organisms, and abiotic stress tolerance. Supporting trade-offs, transcriptome profiling of nutrient-stressed roots revealed differential regulation of several strigolactone biosynthesis and signaling genes in *LGS1*-deficient sorghum compared to a susceptible line. Signatures of balancing selection surrounding *LGS1* and candidates from analysis of genome-wide associations with parasite distribution support long-term maintenance of diversity in parasite resistance genes. Our study of host resistance evolution across smallholder agroecosystems provides a valuable contrast to both industrial farming systems and natural communities.

KEYWORDS: species distribution modeling, environmental niche modeling, genotype-environment association analysis, Red Queen

SIGNIFICANCE STATEMENT:

Understanding co-evolution in crop-parasite systems is critical to management of myriad pests and pathogens confronting modern agriculture. In contrast to wild plant communities, parasites in agricultural ecosystems are usually expected to gain the upper hand in co-evolutionary 'arms races' due to limited genetic diversity of host crops in cultivation. Here, we develop a framework for studying associations between genome diversity in global landraces (traditional varieties) of the staple crop sorghum with the distribution of the devastating parasitic weed *Striga hermonthica.* We find long-term maintenance of diversity in genes related to parasite resistance, highlighting an important role of host adaptation for co-evolutionary dynamics in smallholder agroecosystems.

INTRODUCTION:

Host-parasite interactions can be powerful and dynamic selective forces maintaining genetic variation in natural populations (1). In wild plant pathosystems, long-term balancing selection often maintains diverse resistance alleles in host populations over evolutionary time (2–4). Resistance polymorphism can be maintained by negative frequency-dependent selection, which drives cycling of resistance and virulence alleles when rare alleles provide a selective advantage (i.e. fluctuating Red Queen dynamics *sensu* (5)) (2, 6). Costs of resistance can also generate allele frequency cycles and maintain diversity over gradients of parasite pressure (7).

In contrast to wild plant communities where fluctuating Red Queen dynamics have frequently been observed, low host diversity in agricultural settings is often assumed to permit runaway 'arms races' in fast-evolving parasites (4, 8). Relative to smallholder farms, however, industrial scale farming accounts for a fraction of global production for many food crops (9). The dynamics of host adaptation to parasites across diverse smallholder agricultural systems remains poorly known, despite relevance for identifying novel resistance alleles and managing crop genetic resources (e.g. preserving germplasm both *ex situ* and *in situ*; Jensen et al. 2012). Are co-evolutionary dynamics in smallholder farming systems more similar to natural plant pathosystems, where high connectivity among genetically diverse patches can help promote evolution of host resistance (11)?

Current approaches for identifying and studying the evolution of resistance alleles often involve scoring large panels of diverse individuals (in genome-wide association studies, GWAS) or many recombinant individuals deriving from controlled crosses (in linkage mapping) and using DNA sequence information to identify genomic regions associated with parasite susceptibility. These mapping studies have revealed numerous insights to mechanisms of plant-pathogen dynamics (12), but require extensive phenotyping and genotyping effort for adequate statistical power. To understand the genetic basis of response to abiotic stress, another 'bottom-up' approach is to leverage analysis of the extensive genetic variation present in landraces, traditional crop or livestock varieties which have spread and subsequently adapted to diverse agro-ecological environments following domestication (13–16). Compared to modern improved varieties, which may have lost many resistances due to population bottlenecks and selection for performance in optimal environments (17), landraces and crop wild relatives may be a rich source of alleles conferring resistance to sympatric parasites under a hypothesis of local adaptation to environment of origin. Furthermore, landraces can be studied to test the hypothesis that a natural, putatively environmentally-adapted allele identified from a limited set of experimental environments and genetic backgrounds is indeed adaptive across a wide range of similar environments and across diverse genetic backgrounds (14). Genotype-environment association (GEA) analyses of georeferenced landraces have been a powerful strategy for understanding the genetic basis of local adaptation to gradients of abiotic stressors (14, 15). To our knowledge, similar approaches to investigate adaptation to biotic stress at continent scale have yet to be exploited (but see (16) for an example in Ugandan cattle).

In this study, we extend GEA to biotic gradients to evaluate the frequency and distribution of alleles in genomes of sorghum that confer resistance to *Striga hermonthica* (Delile) Benth., a root-parasitic weed native to Africa. *Sorghum bicolor* (L.) Moench is the world's fifth most important crop and was domesticated from the wild progenitor *Sorghum arundinaceum* (Desv.) Stapf in Africa more than 5000 years ago (18). Sorghum is particularly important in arid and semiarid regions due to its drought tolerance compared to maize and rice. While plant drought responses are influenced by

many processes, in recent years the role of strigolactones, plant hormones that regulate shoot branching (19), root architecture (20) and response to abiotic stress (21), have received particular attention. Strigolactones exuded into the rhizosphere, particularly under nutrient limitation (22) and drought (23), promote interactions with beneficial arbuscular mycorrhizal fungi (24) and are also required as germination stimulants for many root-parasitic plants. In addition to sorghum, *S. hermonthica* attacks maize, rice, millet, sugarcane, and wild grasses and is considered one of the greatest biotic threats to food security in Africa, costing billions of dollars (USD) in crop losses annually through yield loss and abandonment of fields (25).

Here, we evaluate the hypothesis that a geographical selection mosaic across gradients of biotic interactions maintains genetic diversity in *S. hermonthica* resistance in sorghum landraces (26, 27). To identify genomic signatures of host adaptation to parasites, we first develop species distribution models for *S. hermonthica* and search for statistical associations between sorghum genotype and prediction from the parasite model at collection location of each sorghum landrace. We characterize diversity and geographic distribution of loss-of-function alleles at the sorghum resistance gene *LOW GERMINATION STIMULANT 1* (*LGS1*) (28). Loss of *LGS1,* a gene of unknown function with a sulfotransferase domain, alters stereochemistry of the dominant strigolactone in sorghum root exudates, from 5-deoxystrigol to orobanchol, which does not strongly stimulate parasite germination (28, 29). Our ecological genetic analyses of diverse sorghum landraces suggest that *LGS1* loss-of-function mutations are adaptive across a large region of high *S. hermonthica* prevalence in Africa. However, we also present evidence supporting potential trade-offs related to *LGS1* loss-of-function. Because endogenous strigolactones are integral to host plant development, rhizosphere communications, and stress response, we predicted that *LGS1* loss-of-function may adversely impact fitness- or domestication-related traits through altered hormone signaling and perception. We compare root transcriptomes of sorghum lines producing high levels of 5-deoxystrigol or orobanchol to determine if structural variation in SLs impacts expression of strigolactone biosynthesis and signaling pathway components. After focused analyses on *LGS1,* we perform genome-wide tests of association with parasite distribution. We investigate patterns of polymorphism surrounding candidate

147 resistance genes with evidence of locally-adaptive natural variation to determine
148 whether balancing selection has maintained diversity in *S. hermonthica* resistance over
149 evolutionary time.

150 **RESULTS:**

151 S. hermonthica *distribution model*

152 We predicted that host alleles affecting resistance or tolerance would be strongly
153 associated with the geographic distribution of parasites. To identify regions of likely *S.*
154 *hermonthica* occurrence in the absence of continent-wide surveys, we built MaxEnt
155 species distribution models (SDMs) (30). The optimal model showed good ability to
156 predict occurrence with an AUC value of 0.86 (Fig. 1). A high degree of overlap was
157 observed between models generated using all *S. hermonthica* records (*n*=1,050) and a
158 subset of 262 occurrences that were observed specifically in fields of sorghum
159 (Schoener's D = 0.82; I = 0.97). Annual rainfall and total soil N were the most
160 informative variables for predicting *S. hermonthica* occurrence (Table S1). Compared to
161 all cells in the study background, distributions of environmental values for locations with
162 high habitat suitability (HS) were generally restricted to a narrower range of intermediate
163 values of precipitation and soil quality (Fig. S1-2). Locations with the highest HS scores
164 exhibited mean annual rainfall ranging from ~500-1300 mm/year and soil nitrogen
165 ranging from ~400 – 1000 g/kg (10^{th}-90^{th} percentiles for all cells with HS >0.5, Table
166 S1). Soil clay content also contributed substantially to the sorghum-only model, and
167 clay content in locations with the highest HS scores ranged from 12-29% (10^{th}-90^{th}
168 percentile, HS > 0.5, all-occurrence model) or up to 36% (sorghum-only model, Table
169 S1).
170
171 LGS1 *associations with* S. hermonthica *occurrence*

172 We predicted that sorghum resistance alleles would be more common in
173 parasite-prone regions. Evaluating this prediction also allowed us to validate our SDM-
174 based genotype-environment association approach by characterizing associations
175 between *S. hermonthica* distribution and genetic variation at *LGS1*
176 (*Sobic.005G213600*), a known locus causing resistance to *Striga* spp. (28).

Using whole genome sequencing data (~25x coverage) from 143 sorghum landraces, we found evidence for three naturally occurring mutations resulting in *LGS1* loss-of-function (Fig. 2). Two ~30 kb deletions were identified between positions 69,958,377-69,986,892 (*n* = 5 accessions) and 69,981,502-70,011,149 (*n* = 4 accessions, Table S2; Fig. 2A). These two deletions appear to be identical to previously described *lgs1-2* and *lgs1-3* (28), although breakpoint positions reported by our structural variant caller differed slightly. No SNPs in a separate genotyping-by-sequencing (GBS) dataset of >2000 sorghum landraces tagged *lgs1-2* or *lgs1-3* (Fig. S3), and so we imputed large deletions identified from the WGS dataset to the GBS dataset based on patterns of missing data (see Methods). Deletion call imputations were validated by testing root exudate from a subset of sorghum accessions for their ability to induce *S. hermonthica* germination (Fig. S4). We tested four genotypes with likely deletion alleles, and these genotypes stimulated significantly fewer *Striga* seeds to germinate compared to eight other genotypes that did not show strong evidence for deletions (linear mixed-effects model with genotype random effect, deletion genotypes stimulated germination of 8.43 fewer seeds out of 75 total, Wald 95% CI=1.49,15.36). Two of the genotypes stimulated low germination (P721 and SC1439) and had all 14 GBS SNPs missing from *LGS1*, but SNP calls outside of the gene model were inconsistent with *lgs1-2* or *lgs1-3* alleles, perhaps due to the presence of an additional uncharacterized deletion allele.

In addition to *lgs1-2* and *lgs1-3*, we identified a previously unknown high-impact two bp insertion resulting in a frameshift variant in the beginning of the *LGS1* coding region (position 69986146, allele frequency in WGS dataset = 8%). The frameshift was linked to a SNP genotyped in the GBS dataset (T/A at position 69,985,710; D' = 0.93, r^2 = 0.84, Fig. 2B). All nine accessions with the frameshift in the WGS dataset also shared a 315 bp deletion (positions 69,984,268-69,984,583) overlapping 143 bp of the 3' untranslated region in the 1580 bp second exon of *LGS1*.

Although our approach is not well-powered to detect heterozygous deletions or small loss-of-function variants unlinked to SNPs in the GBS dataset, we find evidence that at least three of six independent *LGS1* loss-of-function alleles characterized here and elsewhere (28) are present at low to intermediate frequency. Among accessions

with SNP calls in *LGS1*, 7.0% of accessions exhibited SNP calls consistent with homozygous *lgs1-2* and *lgs1-3* in the GBS dataset (Supplemental Data File S1). Homozygous deletion frequency in African landraces for the GBS dataset was 7.5% compared to 5.3% in non-African landraces. The SNP tagging the frameshift is present at an allele frequency of 15% in the GBS dataset and is found in 16% of African landraces but only 7% of non-African landraces. *LGS1* loss-of-function alleles were found in diverse races and regions for both datasets (Fig. S4, Table S2, Supplemental Data File S1), suggesting that these mutations have had time to spread and that their benefit is not strongly masked by epistasis. Most landrace accessions with *LGS1* deletions and botanical race assignments from the GBS dataset were guinea (12 accessions), caudatum (8 accessions), or durra-caudatum hybrids (17 accessions, Table S2, Supplemental Data File S1).

LGS1 loss-of-function alleles were significantly more common among landraces with high parasite HS scores (Fig. 2C-D). However, correlations with population structure reduced power to detect associations with these resistance alleles after accounting for kinship (Fig. S5). The median *S. hermonthica* HS score was 0.20 for accessions homozygous for *lgs1-2,* 0.54 for accessions homozygous for *lgs1-3,* 0.25 for accession with the frameshift, or 0.09 for accessions without evidence for *LGS1* loss-of-function. The difference in *S. hermonthica* HS score between *lgs1-3* and *LGS1* intact accessions was statistically significant before accounting for relatedness ($p < 0.001$, Wilcoxon rank sum test vs. $p = 0.10$, MLM). Frameshift associations with HS were also statistically significant prior to correction for relatedness ($p < 0.001$, Wilcoxon rank sum; $p = 0.69$, MLM) and were stronger with the sorghum-only model compared to the all-occurrence model ($p = 0.33$, MLM). We observed modest support for associations between *lgs1-2* and *S. hermonthica* HS before correcting for relatedness ($p = 0.06$, Wilcoxon rank sum test; $p = 0.53$, MLM), and stronger associations with the sorghum-only model ($p = 0.26$, MLM).

Upregulation of SL biosynthesis pathway genes in an LGS1-*deficient line*

Changes in strigolactones (and indeed any hormone) are potentially pleiotropic given the many known downstream functions of SLs, suggesting tradeoffs may be

239 associated with *LGS1* variation. We found multiple SL biosynthesis genes were up-
240 regulated in nutrient-stressed roots of a resistant sorghum line (SRN39), which
241 produces high levels of orobanchol, compared to a susceptible sorghum line (Shanqui
242 Red) that produces mainly 5-deoxystrigol (28), a dominant SL in sorghum root exudates
243 that strongly stimulates *S. hermonthica* germination (29). We first confirmed differences
244 in expression for genes located in the *LGS1* region deleted in SRN39. Two gene
245 models in the deletion region were differentially expressed with low expression in
246 Shanqui Red and no reads detected in SRN39 (*Sobic.005G213500*, $p = 0.001$;
247 *Sobic.005G213700*, $p = 0.008$). The two other gene models in the deleted region,
248 *Sobic.005213766* and *Sobic.005213832*, had no reads detected in either line in roots
249 under nutrient stress. *LGS1* was differentially expressed between lines, with low
250 expression in the susceptible line and no expression in SRN39 ($p = 0.03$).
251 In *Arabidopsis* and rice, the strigolactone biosynthesis pathway undergoes
252 negative feedback regulation, in which low strigolactone levels stimulate upregulation of
253 several biosynthesis genes (31, 32). We asked if low endogenous 5-deoxystrigol might
254 also influence SL biosynthesis gene expression in high-orobanchol producing sorghum
255 genotypes. Four of eleven expressed SL biosynthesis genes had higher transcript
256 levels in the *LGS1*-deficient sorghum line SRN39 compared to the susceptible line (Fig.
257 S6, Table S3). These included two genes with homology to *NSP1* (*Sobic.001G341400*,
258 $p < 0.001$ and *Sobic.002G372100*, $p = 0.03$), *CCD7* (*Sobic.006G170300*, $p < 0.001$),
259 and *LBO* (*Sobic.003G418000*, $p = 0.01$). Differences between lines in expression of
260 seven other SL biosynthesis genes were not statistically significant. Among 17 genes
261 with probable roles in SL perception and downstream signaling, *SMXL3*
262 (*Sobic.008G042800*) was differentially expressed between lines and was
263 downregulated in the *LGS1*-deficient line SRN39 ($p = 0.03$). This change in *SMXL3*
264 suggests possible downstream pleiotropy given that regulation of SL-dependent
265 processes such as shoot development and root growth depends on the ubiquitination
266 and degradation of SMXL repressor proteins (33, 34).
267 Overall, 2937 transcripts were differentially expressed in roots of the two lines
268 under nutrient stress. The majority of transcripts were more highly expressed in *LGS1*-
269 deficient line SRN39 compared to *Striga*-susceptible Shanqui Red (1290 downregulated

vs. 1647 upregulated, Supplemental Data File S2). No GO-term was overrepresented among differentially expressed genes, but genes involved in response to a biotic stimulus exhibited the highest enrichment score (GO: 0009607; uncorrected $p = 0.002$; FDR corrected $p = 1$).

Parasite-associated SNPs across the sorghum genome

We performed genome-wide tests of association with predicted parasite HS score. A scan of 317,294 SNPs across 2070 sorghum landraces revealed 97 loci exhibiting significant associations with *S. hermonthica* distribution at a false discovery rate of 5% (Fig. 3A, Table S4). Of SNPs exceeding the threshold for significance, 45 were present within 1 kb of a predicted gene model, and four were predicted to cause an amino acid change (Table S4). Three outlier SNPs were in QTL previously associated with *Striga* resistance (35) including one intron variant in the uncharacterized gene model *Sobic.001G227800* (Table S4). Another outlier SNP was present in an intron of *Sobic.007G090900*, a gene model with high homology to *SMAX1/D53*, which is degraded in an SL-dependent manner to control downstream SL signaling and is associated with tillering and height in rice (36). SNPs among those with the strongest associations to parasite occurrence were also found in genes related to suberin and wax ester biosynthesis (*Sobic.007G091200*) including phenylalanine ammonia-lyase (*Sobic.006G148800*). Phenylalanine ammonia-lyase is highly upregulated in the resistant rice line Nipponbare compared to a susceptible line during infection with *S. hermonthica* (37) and is associated with increased lignin deposition and post-attachment resistance (38).

Across all gene models tagged by SNPs in the genome-wide analysis, no GO term met the threshold for significance after correction for multiple comparisons. The strongest enrichment scores were in genes with GO terms related to cell wall organization (GO:0071555; corrected $p = 0.13$, mean p score for 48 genes = 0.27), cell wall (GO:0005618, corrected $p = 0.17$, mean p score for 70 genes = 0.29), and pectinesterase activity (GO:0030599, corrected $p = 0.22$, mean p score for 39 genes = 0.26). The strongest SNP association to parasite occurrence in a pectinesterase gene model was in *Sobic.002G138400* (SNP S2_21521798, Table S4). The allele associated

with parasite occurrence at S2_21521798 is not predicted to cause an amino acid change, but was in strong linkage disequilibrium (r^2 >0.9) with SNPs up to 204.4 kb upstream of the gene model, which encompasses a region of likely substantial structural variation based on visual inspection of read alignments to the reference. Overall, SNPs in genes related to SL biosynthesis and signaling (Table S3) showed a non-significant enrichment for associations with *S. hermonthica* distribution (uncorrected p = 0.09).

Signatures of selection in candidate regions

We further investigated three candidate genes with polymorphism that exhibited distinct geographic patterns and had known or potential roles in *S. hermonthica* resistance. Elevated Tajima's D values can indicate an excess of shared polymorphism across SNPs at a locus, expected for regions of the genome under balancing selection, whereas strongly negative values can indicate an excess of low frequency polymorphism, expected under either purifying or positive selection. Two 5 kb genomic regions, spanning SNPs in *LGS1* (SNP S5_69986146 in gene model *Sobic.G005G213600*) and a pectinesterase gene (SNP S2_21521798 in gene model *Sobic.002G138400,* MAF=0.275) exhibited elevated values of Tajima's D compared to 1000 randomly sampled 5 kb windows containing or overlapping gene models (Fig. 4; p = 0.06, *Sobic.G005G213600*; p = 0.02, *Sobic.002G138400*). Regions of elevated Tajima's D were localized to relatively small windows centered on SNPs associated with *Striga* habitat suitability, and larger window sizes produced weaker signals (data not shown). We looked for evidence of trans-species polymorphism and found no reads mapping to the pectinesterase gene and no evidence for the *LGS1* loss-of-function alleles characterized in our study in previously sequenced accessions of *S. propinquum* (Kunth) Hitchc. (n=2) and *S. arundinaceum* (as synonym *S. bicolor* subsp. *verticilliflorum* (Steud.) de Wet ex Wiersema & J.Dahlb.) (n=2)(39).

We did not observe strong departures from the neutral expectation for the region surrounding a gene with homology to *SMAX1* (gene model *Sobic.007G090900* tagged by SNP S7_14459084, p=0.6). The minor allele at S7_14459084 was at low frequency in the GBS dataset (MAF = 0.014) and most common in West Africa (Fig. 3C), which is not well sampled in the WGS dataset. The signal of association with *S. hermonthica*

332 occurrence extended more than 7.5 Mb on Chromosome 7 (Fig. 3A), but we did not
333 observe evidence to suggest that S7_14459084 tags an incomplete or soft sweep in
334 either the GBS or WGS datasets according to the haplotype-based statistic nS_L (40).

335 **DISCUSSION:**

336 Pests, pathogens, and parasites threaten human health and food security in a
337 changing world but understanding mechanisms of resistance across diverse taxa
338 remains challenging. Here, we evaluate the hypothesis that geographic selection
339 mosaics maintain genetic diversity in host resistance alleles across gradients of parasite
340 occurrence in smallholder farming systems. We extended genotype-environment
341 association analyses to biotic environmental gradients using species distribution models
342 to model high resolution variation in parasite occurrence at continent scales. We report
343 strong associations with parasite occurrence for novel candidate resistance loci in the
344 sorghum-*Striga hermonthica* pathosystem and characterize diverse loss-of-function
345 mutations in the known sorghum gene *LGS1*. Geographic distribution of loss-of-
346 function alleles suggests that *LGS1*-conferred resistance is stable across environments
347 and genetic backgrounds. However, the intermediate frequency and paucity of *LGS1*
348 loss-of-function alleles outside of parasite-prone areas, combined with *LGS1*-associated
349 changes in sorghum strigolactone biosynthesis and endogenous signaling, suggest
350 there may be trade-offs associated with *LGS1* loss-of-function.

351 Our results support the hypothesis that spatial variation in selective pressures
352 controls geographic clines in the frequency of host resistance alleles. The patterns we
353 characterized are likely representative of long-term averaged conditions as opposed to
354 a snapshot of coevolution because our parasite distribution model used occurrence
355 records spanning more than 150 years, and the landraces we studied were collected
356 across the last several decades. Negative frequency-dependent selection and rapid
357 coevolutionary dynamics, for example, could decouple parasite abundance and the
358 frequency of host resistance alleles. Our approach may be helpful for identifying host
359 alleles whose resistance phenotype is conditional on local parasite genotypes (e.g. as
360 might be suggested by patterns of distribution for polymorphism in *SMAX1*, Fig. 3D).
361 Many parasites including *S. hermonthica* are highly genetically diverse, so that host

362 resistance phenotype differs depending on local parasite genotypes (41). This host by
363 parasite genotype interaction might obscure GWAS for host resistance depending on
364 the parasite genotype used (42). Combining knowledge of parasite population structure
365 with the spatial perspective of parasite-associated host genomic variation presented
366 here could facilitate complementary, inexpensive detection of genomic regions
367 contributing to resistance across diverse biotic environments.

368 Our study revealed evidence for locally-adaptive natural variation in genes
369 related to cell wall modification. Cell-wall modifying enzymes including pectinesterases
370 are highly expressed in the developing haustorium of parasitic plants and in the host-
371 parasite interface (43–46). Pectinesterases de-esterify pectin in plant cell walls, making
372 it accessible to other cell-wall degrading enzymes and loosening cell walls. However,
373 some studies have suggested that in the presence of Ca^{2+}, de-esterified pectin forms
374 egg-box structures and instead stiffens cell walls (47). Rigidification of sorghum cell
375 walls by their own pectinesterases (such as *Sobic.002G138400*, Table S4) or reduced
376 activity could help defend against parasitic invaders. Notably, Yang et al. (2015)
377 reported haustorium specific expression and positive selection on pectinesterase
378 inhibitors in parasitic plant lineages and a pectinesterase inhibitor showed exceptionally
379 high host species-associated expression in field populations of *S. hermonthica* (Lopez-
380 Perez et al., *in press*). Parasite pectinesterase inhibitors could interact with host
381 pectinesterases or help maintain integrity of parasite cell walls in the face of high
382 pectinesterase expression during haustorial invasion. The SNP in a pectinesterase
383 gene most strongly associated with *S. hermonthica* distribution does not code for an
384 amino acid change but is linked with other SNPs across a region spanning substantial
385 structural variation in the WGS dataset, potentially influencing sorghum pectinesterase
386 expression levels during haustorial invasion.

387 Our results also suggest that *LGS1* loss-of-function alleles may be adaptive in *S.*
388 *hermonthica*-prone regions, but that costs of resistance may limit their distribution.
389 Loss-of-function alleles are relatively uncommon but higher in frequency and broadly
390 distributed where parasites occur (Fig. 2C). Associations for the known locus *LGS1*
391 were not statistically significant after correcting for kinship, likely due to covariation with
392 genomic background (Fig. S4), which has been shown to substantially reduce power to

393 detect causal loci in locally-adapted sorghum landraces (14) and in simulations (48).
394 The diversity of loss-of-function variants reported here (Fig. 2A-B) and elsewhere (28),
395 their wide geographic distribution (Fig. 2C), and an excess of high frequency
396 polymorphism localized to *LGS1* (Fig. 4) are consistent with long-term maintenance of
397 *LGS1* diversity under balancing selection. The underlying evolutionary processes
398 remain unknown but could include negative frequency dependent selection or
399 spatiotemporally variable selection favoring different alleles in different environments,
400 depending on the relative costs of resistance (4, 49). Costs of resistance linked to SL
401 structural changes could include the ability to interact with AM fungi, increased
402 susceptibility to other *S. hermonthica* ecotypes more sensitive to orobanchol (e.g. *S.*
403 *hermonthica* that parasitize rice, an orobanchol-exuder), or impacts on endogenous
404 strigolactone signaling. Consistent with the last hypothesis, we find increased
405 expression of SL biosynthesis genes in a sorghum line with low levels of 5-deoxystrigol
406 (5DS), one of the primary SLs produced by sorghum (29, 50). This result could suggest
407 transcriptional feedback in response to deficits in endogenous 5DS in sorghum, as
408 previously observed in *Arabidopsis* and rice in response to low overall SL levels (31,
409 32). Feedback regulation could be mediated by repressors of SL signaling such as
410 SMXL3, a homolog of which was downregulated in the 5DS-deficient line (Table S3).
411 Costs of resistance may also differ among particular loss-of-function alleles, depending
412 on biological pathways influenced by other genes in deleted regions.
413 Another factor potentially contributing to natural variation in SL biosynthesis and
414 signaling is the role of human selection against *S. hermonthica* resistant varieties during
415 domestication and diversification of cultivated sorghum. While impacts of SL structural
416 variation on endogenous function remain poorly known, natural variation in levels of
417 strigolactone production correlates with increased tillering in rice (51, 52), a trait subject
418 to strong selection over the course of cereal domestication (53). One of the most well-
419 studied domestication genes, *Teosinte branched 1 (Tb1)*, controls branching and was a
420 major target of selection during maize domestication (54, 55). *Tb1* activity is decoupled
421 from strigolactone signaling in maize, enabling strigolactone-independent branching
422 regulation (56). However, in pearl millet, signatures of selection on *Tb1* orthologs are
423 weaker (57), consistent with observations that *Tb1* orthologs do not act independently of

strigolactones in other cereals (58). There is also evidence that *Tb1* regulates the maize domestication gene *Teosinte glume architecture 1* (59), a homolog of which also exhibited parasite-associated genetic variation in our study (Table S4).

Taken together, this study provides evidence of locally-adaptive natural variation in sorghum parasite resistance genes across African smallholder farming systems. We report long-term maintenance of diversity in known and novel candidates implicated in pre- and post-attachment resistance to the parasitic plant *Striga hermonthica.* However, the possibility of *LGS1*-driven tradeoffs or the existence of orobanchol-sensitive *S. hermonthica* populations (for example, from rice) suggest potential pitfalls with widespread deployment of the *LGS1* loss-of function allele in sorghum cultivation. Our findings highlight the complexity of interacting abiotic, biotic, and human pressures shaping genome polymorphism across environments in cultivated species.

METHODS:

Species distribution models

Genome-environment association approaches identify putatively locally adaptive genetic loci where allelic variation is strongly associated with home environments (60). To employ this approach with biotic gradients, we required information on local parasite pressure for each sorghum landrace. We used species distribution models (SDMs) to estimate habitat suitability of *Striga hermonthica* at the location of each georeferenced sorghum landrace, under the assumption that modeled habitat suitability scores are a reasonable proxy of parasite success averaged over the long term and in comparison with sites where the parasite never occurs.

S. hermonthica SDMs were constructed with Maxent, a machine learning tool for predicting habitat suitability for a species of interest given a set of environmental variables and presence-only data (30). We compiled 1369 occurrence records for *S. hermonthica* records downloaded from the Global Biodiversity Information Facility (www.gbif.org), newly digitized records for specimens housed in the collections of the Royal Botanic Gardens Kew, the National Museum of Natural History in Paris, the French Agricultural Research Centre for International Development, the University of Montpellier, and the Botanical Garden of Lyon, and observations from published studies

(61–76) (Supplemental Data File S3). Records within 0.01 degree (~1 km) of another observation were excluded to reduce sampling bias. To characterize the background environment across the study extent, we sampled 10,000 points at random from a 500 km radius surrounding locations of 1,050 occurrences in the final dataset. We also created 'sorghum-only' models based on a subset of *S. hermonthica* records (*n* = 262) that were annotated as occurring specifically on sorghum.

Environmental variables were chosen based on prior knowledge of the ecology of *S. hermonthica* (61). Bioclimatic and topographic variables (annual rainfall, mean temperature of the wettest quarter, isothermality, potential evapotranspiration [PET], and topographic wetness index) were obtained from CHELSA (77) and ENVIREM datasets (78). Soil variables (clay content, nitrogen, and phosphorus) were based on continental and global-scale soil property maps (79, 80). We explored additional ecologically relevant variables but did not include them in the final model due to high correlation across the study background with annual rainfall (correlated with soil PH, aluminum, and precipitation seasonality) or soil clay content (correlated with sand fraction) as indicated by Pearson coefficients (|r| >0.7).

SDMs were implemented and evaluated with ENMeval, using the 'checkerboard2' method for data partitioning, which is designed to reduce spatial autocorrelation between testing and training records (81). The distribution model with the lowest ΔAICc was selected for further comparisons with genome variation in sorghum. Two niche overlap statistics, Schoener's *D* (Schoener 1968) and the *I* similarity statistic (83) were calculated for the all-occurrence and sorghum-only models using the R package *dismo* (84).

Sorghum LGS1 *loss-of-function alleles*

Fine-scale natural variation in sorghum *LGS1* was characterized using whole genome sequencing (WGS) data from a set of 143 georeferenced landraces from the sorghum bioenergy association panel (BAP) (85). The BAP includes both sweet and biomass sorghum types, accessions from the five major sorghum botanical races (durra, caudatum, bicolor, guinea, and kafir), and accessions from Africa, Asia, and the Americas. The BAP accessions were sequenced to approximately 25x coverage and

genotyped as part of the TERRA-REF project (www.terraref.org). This whole genome sequencing derived dataset is referred to throughout the manuscript as the 'WGS dataset' to distinguish it from the GBS dataset used for the GEA.

We characterized three loss-of-function alleles in *LGS1* using data from the WGS dataset. Frameshift and nonsense mutations were identified using *SnpEff* v4.3t for SNP calls and small indels in *Sobic.005G213600* available from TERRA-REF (86). High impact variants were manually checked to remove those near the 3' end of the coding region and two linked variants that were present in the same lines and did not cause a frameshift when combined. To characterize large deletion variants, we aligned quality trimmed reads to the *Sorghum bicolor* v3.1 reference genome (DOE-JGI, http://phytozome.jgi.doe.gov/) with BWA MEM v0.7.17 (87). Duplicates were removed with SAMBLASTER v0.1.24 (88) and structural variants were called for each landrace with LUMPY v0.2.13 (89). SVTYPER v0.6.0 was used to call genotypes for structural variants ≤ 1 Mb spanning *Sobic.005G213600* (90).

Following characterization of *LGS1* deletion breakpoints using the WGS dataset, we imputed deletion calls to the GBS dataset. We considered the *LGS1* region to be deleted if at least one SNP was called in the 5 kb region flanking positions of deletion breakpoints, but all data were missing between breakpoints. We considered the LGS1 region to be present if at least one SNP was called within the *Sobic.005G213600* gene model. Fifteen low-coverage samples, with missing data extending 5 kb into flanking regions, were excluded.

Experimental validation of LGS1 *deletion and frameshift alleles*

LGS1 loss-of-function alleles were validated by testing 12 accessions from the Sorghum Association Panel (SAP) (91) for their ability to stimulate *S. hermonthica* germination (Table S5). Three accessions were previously reported as resistant to *S. hermonthica*, two accessions were susceptible, and seven accessions had unknown resistance (28, 92). Root exudates were harvested 43 days after planting (see Supplemental Materials & Methods for a detailed description of plant growth conditions). Germination trials were conducted using seed of *Striga hermonthica* collected on sorghum by Steven Runo (Kenyatta U) in western Kenya and assayed in the USDA

quarantine lab at UVa. Seeds were surface sterilized with 0.5% bleach, rinsed three times with sterile distilled water, and 75 seeds were transferred with 500uL diH_2O to 12-well microtiter plates. After 10 days of preconditioning in the dark at 30^{O}C, 2.25 mL of fresh root exudate was applied to each well. Exudate from five biological replicates (sorghum individuals) per sorghum genotype, with three technical replicates (wells) per biological replicate, were tested. GR24 at two concentrations, 1 ppm and 0.1 ppm, and water were used as positive and negative controls. Germinated seeds were counted under stereomicroscope after 66 hours incubation. We tested significance of deletion alleles using linear mixed effects models in the R package lme4 (93), where deletion was a fixed effect and genotypes were random effects.

LGS1 and expression of genes in strigolactone synthesis and signaling pathways

To assess the impact of putatively locally adaptive variation at *LGS1*, we studied root transcriptomes of two lines segregating for presence/absence. We generated TagSeq libraries using root tissue from five replicate individuals each of sorghum lines Shanqui Red (PI 656025) and SRN39 (PI 656027), grown under nutrient deficient conditions. Shanqui Red is susceptible to *S. hermonthica*, whereas SRN39 is resistant as a result of a ~34 kb deletion spanning *LGS1* and four adjacent genes (28). Five replicates of each line were grown under identical conditions as for root exudate collection. Twenty-five days after planting, all potting components were carefully washed from roots, and 2-5 ml of the fine root tissue was sampled, placed into labeled vials and stored on ice for 1 day during shipment to U of Texas, where samples were stored at -80°C until RNA extraction.

RNA extractions were performed with TRIzol Reagent after grinding root tissues in liquid nitrogen using mortar and pestle. We used the 3'-TagSeq approach (94) with several modifications to construct cDNA libraries. This method focuses on the 3' end of transcripts enriched in a size range of 400-500 bp fragments.

cDNA libraries were sequenced on a single lane of an Illumina Hiseq-2500 analyzer at the Genomic Sequencing and Analysis Facility at the University of Texas at Austin. We recovered between 3 to 5 million raw single-end 150 bp reads per sample and compared expression differences between SRN39 and Shanqui Red using the TagSeq

v2.0 pipeline (https://github.com/Eli-Meyer/TagSeq_utilities/). A detailed description of the library preparation method and bioinformatic analysis is given in Supplemental Materials & Methods.

Count data were analyzed in DESeq2 with FDR correction (α=0.05) (95). Enrichment analysis was performed as for genome-wide association analysis, except only the set of gene models with non-zero expression were used as the background.

Genome-environment associations

We performed a genome-wide scan for SNPs in the sorghum genome strongly associated with values of habitat suitability estimated by our *S. hermonthica* distribution model. Sorghum genotypic information was extracted from a public dataset of accessions genotyped using genotyping-by-sequencing (GBS) (14, 96–98). This dataset comprises a diverse set of worldwide accessions including germplasm from the SAP (91), the Mini-Core Collection (99), and the Bioenergy Association Panel (BAP) (85). Beagle 4.1 was used to impute missing data based on the Li and Stephens (2003) haplotype frequency model (100). The average missing rate in the non-imputed dataset is 0.39 (98). After excluding sorghum accessions with missing coordinates and SNPs with minor allele frequency less than 0.01, the dataset, hereafter referred to as the 'GBS dataset', included 1547 African landraces among 2070 georeferenced accessions total genotyped at 317,294 SNPs. At each location of a georeferenced accession in the GBS dataset, we extracted logistic output from the *S. hermonthica* distribution model (Supplemental Data File S4-5) as the 'phenotype'. To account for regions where predicted habitat suitability is high but *S. hermonthica* has not been recorded, we cropped model predictions to within 200 km from any occurrence record and set values outside of this range to zero to derive for each grid cell an *S. hermonthica* occurrence score ranging from zero to one; more than half of sorghum accessions are from locations with parasite HS scores greater than zero (Fig. 1B). Genome-wide associations for each SNP with *S. hermonthica* occurrence were computed for the GBS dataset using a mixed linear model (MLM) fit with GEMMA v0.94 (101). To take into account relatedness among individuals, we used a centered kinship matrix (-gk 1) generated from all 317,294 SNPs before calculation of p score statistics (-lmm 3). P

578 scores were adjusted for multiple comparisons using the Benjamini and Hochberg
579 (1995) procedure (FDR = 0.05). To visualize genomic regions previously implicated in
580 resistance to *S. hermonthica,* locations of QTL from Haussman et al. (2004) in the *S.*
581 *bicolor* v3.0 genome were downloaded from the Sorghum QTL Atlas
582 (http://aussorgm.org.au) (102). We tested for associations with *LGS1* loss-of-function
583 mutations using the same procedure and kinship matrix as for the genome-wide
584 association analysis.
585 We identified gene functions enriched for associations with parasite distribution
586 using the gene score resampling method in ErmineJ (103). This method places higher
587 value on gene scores than their relative ranking and does not require choice of a
588 threshold for significance. For each gene model, we used the lowest p score from
589 GEMMA of any SNP within 1 kb of gene model boundaries, and enrichment analyses
590 were performed using the mean of all gene scores in the gene set. Gene sets were
591 created using GO terms for all gene models in the *Sorghum bicolor* v3.0 genome
592 (annotation version 3.1). We also created a custom gene set comprising 30 gene
593 models implicated in strigolactone biosynthesis and signaling (Table S3). This gene set
594 included nine gene models annotated as belonging to Phytozome pathway Sbicolor
595 PWY-7101 (*D27*, *CCD7*, and *CCD8* homologs), and all sorghum gene models
596 annotated with best BLASTP hits to Arabidopsis *MAX1*, *LBO* (104), *AtD14, SMAX1,*
597 *SMXL3/4/5/6/7, NSP1,* and *NSP2* (105). Enrichment analysis was performed with
598 200,000 iterations, excluding gene sets with less than 5 or more than 200 genes.
599
600 *Signatures of selection in candidate genomic regions*
601 We predicted functional impacts for candidate SNPs of interest and performed
602 scans for selection in 1 Mb regions surrounding each focal SNP. Linkage disequilibrium
603 between sites was determined with vcftools v0.1.15 (--geno-r2 parameter). To identify
604 regions under balancing selection among a subset of African landraces, we used
605 Tajima's D calculated with vcftools in non-overlapping 5 kb windows, excluding SNPs
606 with more than 70% missing data. *P*-values for candidate regions under selection were
607 calculated based on the empirical distribution of Tajima's D for 1000 randomly sampled

608 5 kb windows that overlapped or fully encompassed gene models. We searched for
609 sweeps using the nS$_L$ statistic with selscan v1.2.0a (106).
610
611 **Acknowledgments**
612 We thank the many collectors, volunteers, and herbarium curators who made this work
613 possible and are particularly grateful to Marie-Hélène Weech and the staff of the Royal
614 Botanic Gardens Kew and the Muséum national d'Histoire naturelle. We thank Steven
615 Runo for providing *S. hermonthica* seeds and Alice MacQueen for comments that
616 improved the manuscript. Whole genome sequence data used here is from the TERRA
617 REF experiment, funded by the Advanced Research Projects Agency-Energy (ARPA-
618 E), U.S. Department of Energy, under Award Number DE-AR0000594. This material is
619 based on work supported by a National Science Foundation Postdoctoral Research
620 Fellowship in Biology to ESB under Grant No. 1711950. The views and opinions of
621 authors expressed herein do not necessarily state or reflect those of the United States
622 Government or any agency thereof.
623

624 **FIGURES:**

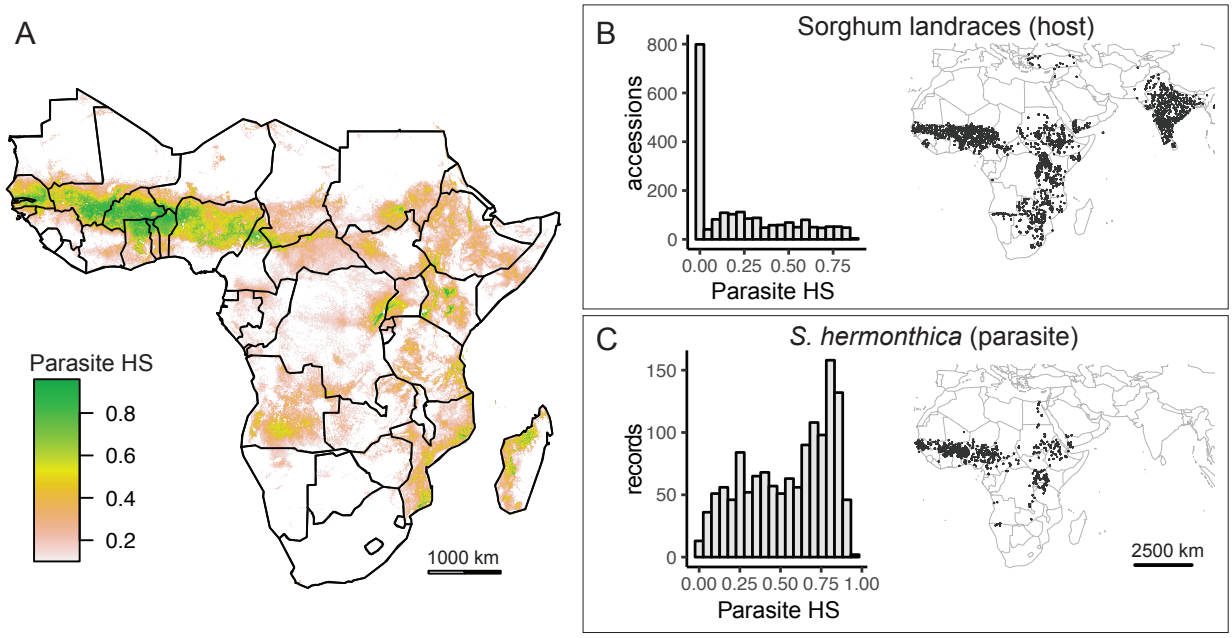

625

626 **Fig. 1:** A subset of global sorghum landraces are from parasite-prone areas. A) *Striga*
627 *hermonthica* habitat suitability (HS) scores across Africa based on MaxEnt species
628 distribution model. B) Geographic distribution and frequency histogram of HS scores at
629 locations of 2070 georeferenced and genotyped sorghum landrace accessions. To
630 account for areas with high HS where parasites have not been recorded, HS for
631 accessions more than 200 km from any *S. hermonthica* record was set to zero. C)
632 Geographic distribution and frequency histogram of HS scores at locations of 1369 *S.*
633 *hermonthica* occurrence records.

634

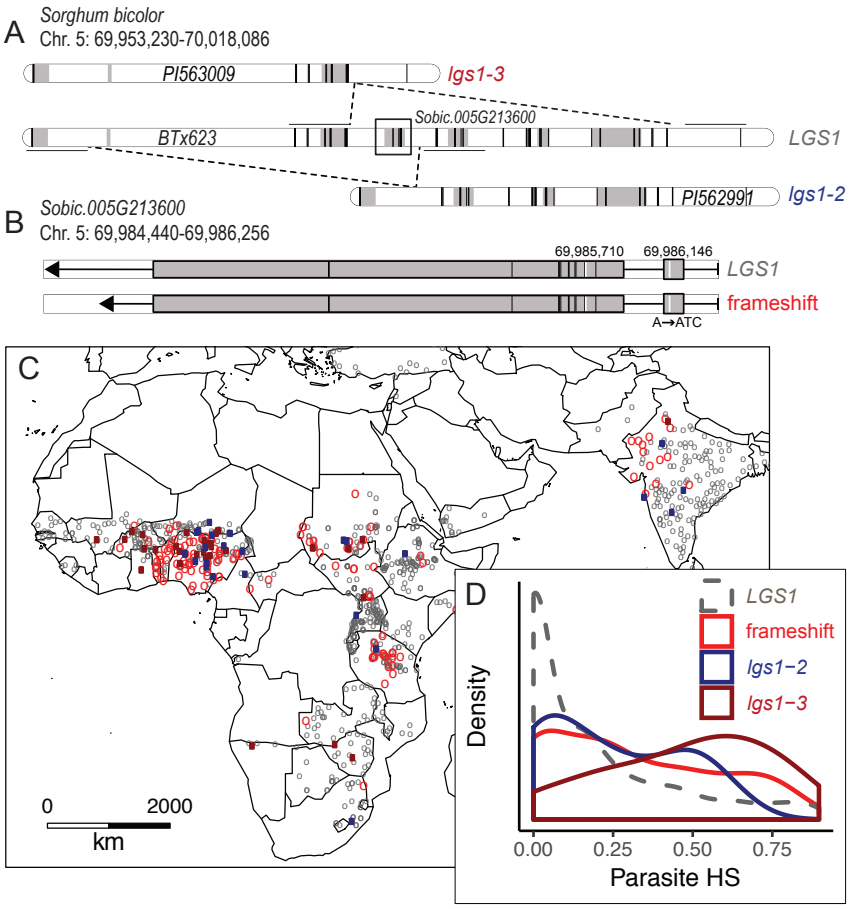

Fig. 2. *LGS1* loss-of-function alleles are broadly distributed within parasite-prone regions. Schematic of large deletion variants (A) and frameshift mutation (B) impacting sorghum *LGS1*, a known locus involved in resistance to *Striga* spp. Grey shading indicates position of gene models (A) or coding regions (B). Position of SNPs in the GBS dataset is indicated by vertical black bars, and horizontal black lines denote 5 kb flanking regions used to impute deletion calls. In B, vertical white bars show the frameshift mutation (position 69,986,146) and the SNP at position 69,985,710 that tags the frameshift in the GBS dataset. C) Geographic distribution of *LGS1* alleles in sorghum landraces. D) Distribution of parasite habitat suitability (HS) scores at locations of sorghum accessions with *lgs1-2* (*n*=25), *lgs1-3* (*n*=34), frameshift (*n*=131), or intact *LGS1* (*n*=785).

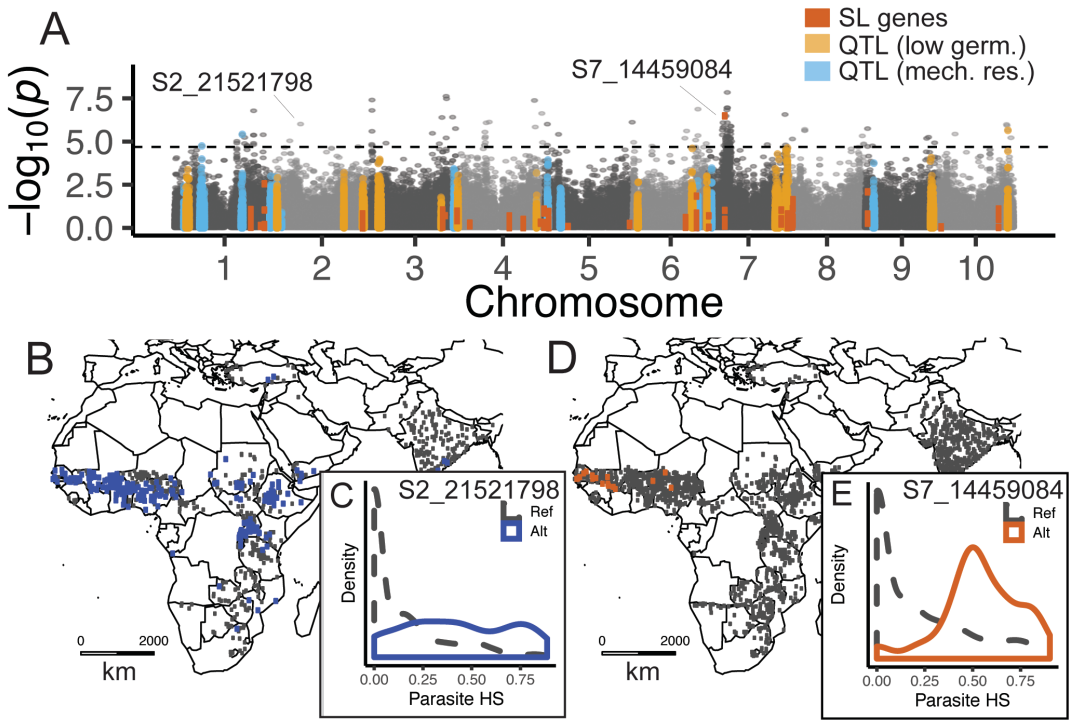

Fig. 3: Sorghum genome-wide associations with parasite distribution implicate cell-wall and strigolactone signaling genes. A) Genome-wide association with parasite habitat suitability (HS) score, based on 317,294 SNPs with minor allele frequency (MAF) > 0.01 in 2070 sorghum landraces. SNPs in genomic regions linked to strigolactone (SL) biosynthesis/signaling (red), mechanical resistance (light blue), or low *Striga hermonthica* germination (orange) are indicated. The dashed line represents significance threshold at a false discovery rate of 5%. B) Geographic distribution of reference and alternate alleles for a SNP (S2_21521798) in a pectinesterase gene (MAF = 0.275). C) Distribution of parasite habitat suitability scores for sorghum accessions segregating for S2_21521798. D) Geographic distribution of reference and alternate alleles for a SNP (S7_14459084) in a gene homologous to SMAX1 (MAF = 0.014). E) Distribution of parasite HS scores for sorghum accessions segregating for S7_14459084.

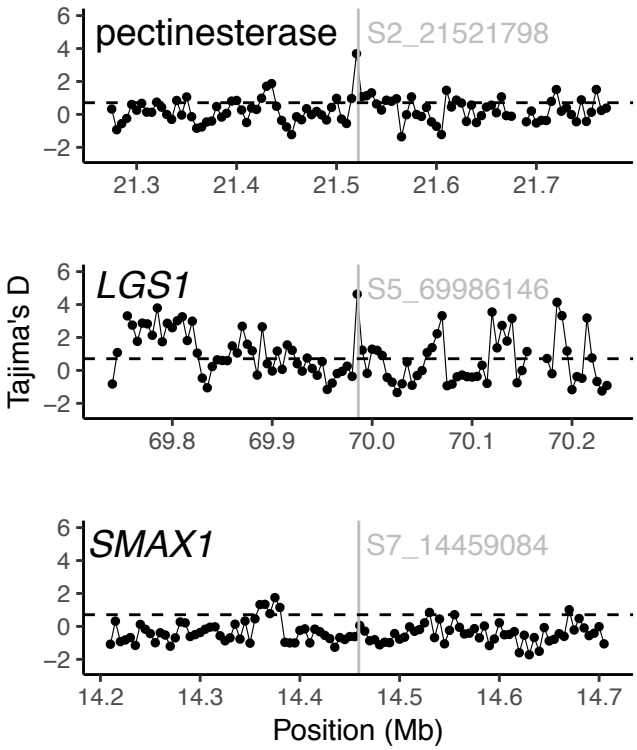

664

665 **Fig. 4. Signatures of balancing selection surround parasite-associated SNPs in a**
666 **pectinesterase gene (S2_21521798) and *LGS1* (S5_69986146).** The region
667 surrounding a SNP in a gene homologous to *SMAX1* (S7_14459084, lower panel) is
668 also shown. Tajima's D was calculated in non-overlapping windows of 5 kb using data
669 from the WGS dataset subset to 143 African landraces. The dashed horizontal line
670 indicates the median value for 1000 randomly selected 5 kb windows overlapping or
671 encompassing gene models. Vertical grey lines indicate positions of the CDS location
672 for the gene containing the focal SNP.

673 **REFERENCES:**

674 1. Haldane JBS (1949) Disease and Evolution. *Ricerca Scientifica* 19:68–76.

675 2. Stahl EA, Dwyer G, Mauricio R, Kreitman M, Bergelson J (1999) Dynamics of disease
676 resistance polymorphism at the Rpm1 locus of Arabidopsis. *Nature* 400(6745):667–671.

677 3. Tack AJM, Thrall PH, Barrett LG, Burdon JJ, Laine A-L (2012) Variation in infectivity and
678 aggressiveness in space and time in wild host-pathogen systems: causes and
679 consequences. *Journal of Evolutionary Biology* 25(10):1918–1936.

680 4. Karasov TL, Horton MW, Bergelson J (2014) Genomic variability as a driver of plant–
681 pathogen coevolution? *Current Opinion in Plant Biology* 18:24–30.

682 5. Brockhurst MA, et al. (2014) Running with the Red Queen: the role of biotic conflicts in
683 evolution. *Proceedings of the Royal Society B: Biological Sciences* 281(1797):20141382.

684 6. Bergelson J, Dwyer G, Emerson JJ (2001) Models and Data on Plant-Enemy Coevolution.
685 *Annual Review of Genetics* 35(1):469–499.

686 7. Agrawal A, Lively CM (2002) Infection genetics: gene-for-gene versus matching- alleles
687 models and all points in between. *Evolutionary Ecology Research* 4:79–90.

688 8. Möller M, Stukenbrock EH (2017) Evolution and genome architecture in fungal plant
689 pathogens. *Nature Reviews Microbiology* 15(12):756–771.

690 9. Samberg LH, Gerber JS, Ramankutty N, Herrero M, West PC (2016) Subnational
691 distribution of average farm size and smallholder contributions to global food production.
692 *Environ Res Lett* 11(12):124010.

693 10. Jensen HR, Dreiseitl A, Sadiki M, Schoen DJ (2012) The Red Queen and the seed bank:
694 pathogen resistance of *ex situ* and *in situ* conserved barley. *Evolutionary Applications*
695 5(4):353–367.

696 11. Jousimo J, et al. (2014) Ecological and evolutionary effects of fragmentation on infectious
697 disease dynamics. *Science* 344(6189):1289–1293.

698 12. Bartoli C, Roux F (2017) Genome-Wide Association Studies In Plant Pathosystems:
699 Toward an Ecological Genomics Approach. *Front Plant Sci* 8.
700 doi:10.3389/fpls.2017.00763.

701 13. Meyer RS, Purugganan MD (2013) Evolution of crop species: genetics of domestication
702 and diversification. *Nature Reviews Genetics* 14(12):840–852.

703 14. Lasky JR, et al. (2015) Genome-environment associations in sorghum landraces predict
704 adaptive traits. *Science Advances* 1(6):e1400218.

705 15. Romero Navarro JA, et al. (2017) A study of allelic diversity underlying flowering-time
706 adaptation in maize landraces. *Nature Genetics* 49(3):476–480.

16. Vajana E, et al. (2018) Combining Landscape Genomics and Ecological Modelling to Investigate Local Adaptation of Indigenous Ugandan Cattle to East Coast Fever. *Front Genet* 9. doi:10.3389/fgene.2018.00385.

17. Gaillard MDP, Glauser G, Robert CAM, Turlings TCJ (2018) Fine-tuning the "plant domestication-reduced defense" hypothesis: specialist vs generalist herbivores. *New Phytol* 217(1):355–366.

18. Winchell F, Stevens CJ, Murphy C, Champion L, Fuller DorianQ (2017) Evidence for Sorghum Domestication in Fourth Millennium BC Eastern Sudan: Spikelet Morphology from Ceramic Impressions of the Butana Group. *Current Anthropology* 58(5):673–683.

19. Gomez-Roldan V, et al. (2008) Strigolactone inhibition of shoot branching. *Nature* 455(7210):189–194.

20. Ruyter-Spira C, et al. (2011) Physiological Effects of the Synthetic Strigolactone Analog GR24 on Root System Architecture in Arabidopsis: Another Belowground Role for Strigolactones? *Plant Physiology* 155(2):721–734.

21. Ha CV, et al. (2014) Positive regulatory role of strigolactone in plant responses to drought and salt stress. *Proc Natl Acad Sci U S A* 111(2):851–856.

22. Yoneyama K, et al. (2007) Nitrogen deficiency as well as phosphorus deficiency in sorghum promotes the production and exudation of 5-deoxystrigol, the host recognition signal for arbuscular mycorrhizal fungi and root parasites. *Planta* 227(1):125–132.

23. Ruiz-Lozano JM, et al. (2016) Arbuscular mycorrhizal symbiosis induces strigolactone biosynthesis under drought and improves drought tolerance in lettuce and tomato. *Plant, Cell & Environment* 39(2):441–452.

24. Akiyama K, Matsuzaki K, Hayashi H (2005) Plant sesquiterpenes induce hyphal branching in arbuscular mycorrhizal fungi. *Nature* 435:824–827.

25. Spallek T, Mutuku M, Shirasu K (2013) The genus *Striga*: a witch profile. *Molecular Plant Pathology* 14(9):861–869.

26. Laine A-L (2004) Resistance variation within and among host populations in a plant–pathogen metapopulation: implications for regional pathogen dynamics. *Journal of Ecology* 92(6):990–1000.

27. Thompson JN (1999) Specific Hypotheses on the Geographic Mosaic of Coevolution. *The American Naturalist* 153(S5):S1–S14.

28. Gobena D, et al. (2017) Mutation in sorghum LOW GERMINATION STIMULANT 1 alters strigolactones and causes *Striga* resistance. *PNAS* 114(17):4471–4476.

29. Mohemed N, et al. (2018) Genetic variation in *Sorghum bicolor* strigolactones and their role in resistance against *Striga hermonthica*. *J Exp Bot* 69(9):2415–2430.

30. Phillips SJ, Anderson RP, Schapire RE (2006) Maximum entropy modeling of species geographic distributions. *Ecological Modelling* 190(3–4):231–259.

744 31. Arite T, et al. (2007) DWARF10, an RMS1/MAX4/DAD1 ortholog, controls lateral bud
745 outgrowth in rice. *Plant J* 51(6):1019–1029.

746 32. Mashiguchi K, et al. (2009) Feedback-Regulation of Strigolactone Biosynthetic Genes and
747 Strigolactone-Regulated Genes in Arabidopsis. *Bioscience, Biotechnology, and*
748 *Biochemistry* 73(11):2460–2465.

749 33. Wallner E-S, et al. (2017) Strigolactone- and Karrikin-Independent SMXL Proteins Are
750 Central Regulators of Phloem Formation. *Current Biology* 27(8):1241–1247.

751 34. Wang L, et al. (2015) Strigolactone Signaling in Arabidopsis Regulates Shoot Development
752 by Targeting D53-Like SMXL Repressor Proteins for Ubiquitination and Degradation.
753 *Plant Cell* 27(11):3128–3142.

754 35. Haussmann BIG, et al. (2004) Genomic regions influencing resistance to the parasitic
755 weed *Striga hermonthica* in two recombinant inbred populations of sorghum. *Theor Appl*
756 *Genet* 109(5):1005–1016.

757 36. Jiang L, et al. (2013) DWARF 53 acts as a repressor of strigolactone signalling in rice.
758 *Nature* 504(7480):401–405.

759 37. Swarbrick PJ, et al. (2008) Global patterns of gene expression in rice cultivars undergoing
760 a susceptible or resistant interaction with the parasitic plant *Striga hermonthica*. *New*
761 *Phytol* 179(2):515–529.

762 38. Mutuku JM, et al. (2019) The structural integrity of lignin is crucial for resistance against
763 *Striga hermonthica* parasitism in rice. *Plant Physiology*:pp.01133.2018.

764 39. Mace ES, et al. (2013) Whole-genome sequencing reveals untapped genetic potential in
765 Africa's indigenous cereal crop sorghum. *Nature Communications* 4:2320.

766 40. Ferrer-Admetlla A, Liang M, Korneliussen T, Nielsen R (2014) On Detecting Incomplete
767 Soft or Hard Selective Sweeps Using Haplotype Structure. *Mol Biol Evol* 31(5):1275–
768 1291.

769 41. Soltis NE, et al. (2019) Interactions of Tomato and *Botrytis cinerea* Genetic Diversity:
770 Parsing the Contributions of Host Differentiation, Domestication, and Pathogen Variation.
771 *The Plant Cell* 31(2):502–519.

772 42. MacPherson A, Otto SP, Nuismer SL (2018) Keeping Pace with the Red Queen:
773 Identifying the Genetic Basis of Susceptibility to Infectious Disease. *Genetics* 208(2):779–
774 789.

775 43. Honaas LA, et al. (2013) Functional genomics of a generalist parasitic plant: Laser
776 microdissection of host-parasite interface reveals host-specific patterns of parasite gene
777 expression. *BMC Plant Biology* 13(1):9.

778 44. Yang Z, et al. (2015) Comparative Transcriptome Analyses Reveal Core Parasitism Genes
779 and Suggest Gene Duplication and Repurposing as Sources of Structural Novelty. *Mol*
780 *Biol Evol* 32(3):767–790.

781 45. Sun G, et al. (2018) Large-scale gene losses underlie the genome evolution of parasitic
782 plant *Cuscuta australis*. *Nature Communications* 9(1):2683.

783 46. Losner-Goshen D, Portnoy VH, Mayer AM, Joel DM (1998) Pectolytic Activity by the
784 Haustorium of the Parasitic Plant *Orobanche* L. (Orobanchaceae) in Host Roots. *Ann Bot*
785 81(2):319–326.

786 47. Hocq L, Pelloux J, Lefebvre V (2017) Connecting Homogalacturonan-Type Pectin
787 Remodeling to Acid Growth. *Trends in Plant Science* 22(1):20–29.

788 48. Forester BR, Lasky JR, Wagner HH, Urban DL (2018) Comparing methods for detecting
789 multilocus adaptation with multivariate genotype–environment associations. *Molecular*
790 *Ecology* 27(9):2215–2233.

791 49. Brisson D (2018) Negative Frequency-Dependent Selection Is Frequently Confounding.
792 *Front Ecol Evol* 6. doi:10.3389/fevo.2018.00010.

793 50. Awad AA, et al. (2006) Characterization of Strigolactones, Germination Stimulants for the
794 Root Parasitic Plants *Striga* and *Orobanche*, Produced by Maize, Millet and Sorghum.
795 *Plant Growth Regul* 48(3):221.

796 51. Jamil M, Charnikhova T, Houshyani B, van Ast A, Bouwmeester HJ (2012) Genetic
797 variation in strigolactone production and tillering in rice and its effect on *Striga*
798 *hermonthica* infection. *Planta* 235(3):473–484.

799 52. Cardoso C, et al. (2014) Natural variation of rice strigolactone biosynthesis is associated
800 with the deletion of two MAX1 orthologs. *PNAS* 111(6):2379–2384.

801 53. Doust A (2007) Architectural evolution and its implications for domestication in grasses.
802 *Ann Bot* 100(5):941–950.

803 54. Studer A, Zhao Q, Ross-Ibarra J, Doebley J (2011) Identification of a functional transposon
804 insertion in the maize domestication gene *tb1*. *Nature Genetics* 43(11):1160–1163.

805 55. Wang RL, Stec A, Hey J, Lukens L, Doebley J (1999) The limits of selection during maize
806 domestication. *Nature* 398(6724):236–239.

807 56. Guan JC, et al. (2012) Diverse Roles of Strigolactone Signaling in Maize Architecture and
808 the Uncoupling of a Branching-Specific Subnetwork. *Plant Physiology* 160(3):1303–1317.

809 57. Remigereau M-S, et al. (2011) Cereal Domestication and Evolution of Branching: Evidence
810 for Soft Selection in the Tb1 Orthologue of Pearl Millet (*Pennisetum glaucum* [L.] R. Br.).
811 *PLOS ONE* 6(7):e22404.

812 58. Minakuchi K, et al. (2010) FINE CULM1 (FC1) Works Downstream of Strigolactones to
813 Inhibit the Outgrowth of Axillary Buds in Rice. *Plant Cell Physiol* 51(7):1127–1135.

814 59. Studer AJ, Wang H, Doebley JF (2017) Selection During Maize Domestication Targeted a
815 Gene Network Controlling Plant and Inflorescence Architecture. *Genetics* 207(2):755–
816 765.

817 60. Rellstab C, Gugerli F, Eckert AJ, Hancock AM, Holderegger R (2015) A practical guide to
818 environmental association analysis in landscape genomics. *Molecular Ecology*
819 24(17):4348–4370.

820 61. Mohamed KI, Musselman LJ, Riches CR (2001) The Genus *Striga* (Scrophulariaceae) in
821 Africa. *Annals of the Missouri Botanical Garden* 88(1):60–103.

822 62. Gethi JG, Smith ME, Mitchell SE, Kresovich S (2005) Genetic diversity of *Striga*
823 *hermonthica* and *Striga asiatica* populations in Kenya. *Weed Research* 45(1):64–73.

824 63. Olivier A, Glaszmann J-C, Lanaud C, Leroux GD (1998) Population structure, genetic
825 diversity and host specificity of the parasitic weed *Striga hermonthica* (Scrophulariaceae)
826 in Sahel. *Pl Syst Evol* 209(1):33–45.

827 64. Bozkurt ML, Muth P, Parzies HK, Haussmann BIG (2015) Genetic diversity of East and
828 West African *Striga hermonthica* populations and virulence effects on a contrasting set of
829 sorghum cultivars. *Weed Research* 55(1):71–81.

830 65. Unachukwu NN, et al. (2017) Genetic diversity and population structure of *Striga*
831 *hermonthica* populations from Kenya and Nigeria. *Weed Research* 57(5):293–302.

832 66. Estep MC, et al. (2011) Genetic Diversity of a Parasitic Weed, *Striga hermonthica*, on
833 Sorghum and Pearl Millet in Mali. *Tropical Plant Biol* 4(2):91–98.

834 67. Samejima H, Babiker AG, Mustafa A, Sugimoto Y (2016) Identification of *Striga*
835 *hermonthica*-Resistant Upland Rice Varieties in Sudan and Their Resistance Phenotypes.
836 *Front Plant Sci* 7:634.

837 68. Mohemed N, et al. (2016) Evaluation of field resistance to Striga hermonthica (Del.) Benth.
838 in Sorghum bicolor (L.) Moench. The relationship with strigolactones. *Pest Manag Sci*
839 72(11):2082–2090.

840 69. Tarr SAJ (1961) Witchweed (*Striga hermonthica*) on rain-grown pearl millet in nitrogen-
841 deficient sandy soil of the central Sudan. *Annals of Applied Biology* 49(2):347–349.

842 70. Yohannes T, et al. (2015) Marker-assisted introgression improves *Striga resistance* in an
843 Eritrean Farmer-Preferred Sorghum Variety. *Field Crops Research* 173:22–29.

844 71. Joel KA, Runo S, Muchugi A (2018) Genetic diversity and virulence of *Striga hermonthica*
845 from Kenya and Uganda on selected sorghum varieties. *1* 10(2):111–120.

846 72. Mrema E, Shimelis H, Laing M, Bucheyeki T (2017) Screening of sorghum genotypes for
847 resistance to *Striga hermonthica* and *S. asiatica* and compatibility with *Fusarium*
848 *oxysporum* f.sp. *strigae*. *Acta Agriculturae Scandinavica, Section B — Soil & Plant*
849 *Science* 67(5):395–404.

850 73. Abate M, Hussien T, Bayu W, Reda F (2017) Diversity in root traits of sorghum genotypes
851 in response to *Striga hermonthica* infestation. *Weed Research* 57(5):303–313.

852 74. Bebawi FF (1981) Intraspecific Physiological Variants of *Striga hermonthica*. *Experimental*
853 *Agriculture* 17(4):419–423.

854 75. Welsh AB, Mohamed KI (2011) Genetic Diversity of *Striga hermonthica* Populations in
855 Ethiopia: Evaluating the Role of Geography and Host Specificity in Shaping Population
856 Structure. *International Journal of Plant Sciences* 172(6):773–782.

857 76. Gbèhounou G, Pieterse AH, Verkleij JAC (2000) Endogenously induced secondary
858 dormancy in seeds of *Striga hermonthica*. *Weed Science* 48(5):561–566.

859 77. Karger DN, et al. (2017) Climatologies at high resolution for the earth's land surface areas.
860 *Scientific Data* 4:170122.

861 78. Title PO, Bemmels JB (2018) ENVIREM: an expanded set of bioclimatic and topographic
862 variables increases flexibility and improves performance of ecological niche modeling.
863 *Ecography* 41(2):291–307.

864 79. Hengl T, et al. (2017) SoilGrids250m: Global gridded soil information based on machine
865 learning. *PLOS ONE* 12(2):e0169748.

866 80. Hengl T, et al. (2017) Soil nutrient maps of Sub-Saharan Africa: assessment of soil nutrient
867 content at 250 m spatial resolution using machine learning. *Nutr Cycl Agroecosyst*
868 109(1):77–102.

869 81. Muscarella R, et al. (2014) ENMeval: An R package for conducting spatially independent
870 evaluations and estimating optimal model complexity for Maxent ecological niche models.
871 *Methods in Ecology and Evolution* 5(11):1198–1205.

872 82. Schoener TW (1968) The Anolis Lizards of Bimini: Resource Partitioning in a Complex
873 Fauna. *Ecology* 49(4):704–726.

874 83. Warren DL, Glor RE, Turelli M (2008) Environmental niche equivalency versus
875 conservatism: quantitative approaches to niche evolution. *Evolution* 62(11):2868–2883.

876 84. Hijmans RJ, Phillips S, Elith JL and J (2017) *dismo: Species Distribution Modeling*
877 Available at: https://CRAN.R-project.org/package=dismo [Accessed March 28, 2019].

878 85. Brenton ZW, et al. (2016) A Genomic Resource for the Development, Improvement, and
879 Exploitation of Sorghum for Bioenergy. *Genetics* 204(1):21–33.

880 86. Cingolani P, et al. (2012) A program for annotating and predicting the effects of single
881 nucleotide polymorphisms, SnpEff: SNPs in the genome of *Drosophila melanogaster*
882 *strain* w^{1118}; iso-2; iso-3. *Fly* 6(2):80–92.

883 87. Li H, Durbin R (2009) Fast and accurate short read alignment with Burrows-Wheeler
884 transform. *Bioinformatics* 25(14):1754–1760.

885 88. Faust GG, Hall IM (2014) SAMBLASTER: fast duplicate marking and structural variant
886 read extraction. *Bioinformatics* 30(17):2503–2505.

887 89. Layer RM, Chiang C, Quinlan AR, Hall IM (2014) LUMPY: a probabilistic framework for
888 structural variant discovery. *Genome Biology* 15(6):R84.

889 90. Chiang C, et al. (2015) SpeedSeq: ultra-fast personal genome analysis and interpretation.
890 *Nature Methods* 12(10):966–968.

891 91. Casa AM, et al. (2008) Community Resources and Strategies for Association Mapping in
892 Sorghum. *Crop Science* 48(1):30–40.

893 92. Hess DE, Ejeta G, Butler LG (1992) Selecting sorghum genotypes expressing a
894 quantitative biosynthetic trait that confers resistance to Striga. *Phytochemistry* 31(2):493–
895 497.

896 93. Bates D, Mächler M, Bolker B, Walker S (2015) Fitting Linear Mixed-Effects Models Using
897 lme4. *Journal of Statistical Software* 67(1):1–48.

898 94. Meyer E, Aglyamova GV, Matz MV (2011) Profiling gene expression responses of coral
899 larvae (Acropora millepora) to elevated temperature and settlement inducers using a
900 novel RNA-Seq procedure. *Molecular Ecology* 20(17):3599–3616.

901 95. Love MI, Huber W, Anders S (2014) Moderated estimation of fold change and dispersion
902 for RNA-seq data with DESeq2. *Genome Biology* 15(12):550.

903 96. Elshire RJ, et al. (2011) A Robust, Simple Genotyping-by-Sequencing (GBS) Approach for
904 High Diversity Species. *PLOS ONE* 6(5):e19379.

905 97. Morris GP, et al. (2013) Population genomic and genome-wide association studies of
906 agroclimatic traits in sorghum. *Proceedings of the National Academy of Sciences*
907 110(2):453–458.

908 98. Hu Z, Olatoye MO, Marla S, Morris GP (2019) An Integrated Genotyping-by-Sequencing
909 Polymorphism Map for Over 10,000 Sorghum Genotypes. *The Plant Genome* 12(1):0.

910 99. Upadhyaya HD, et al. (2009) Developing a Mini Core Collection of Sorghum for Diversified
911 Utilization of Germplasm. *Crop Science* 49(5):1769–1780.

912 100. Browning BL, Browning SR (2016) Genotype Imputation with Millions of Reference
913 Samples. *Am J Hum Genet* 98(1):116–126.

914 101. Zhou X, Stephens M (2012) Genome-wide efficient mixed-model analysis for association
915 studies. *Nat Genet* 44(7):821–824.

916 102. Mace E, et al. (2018) The Sorghum QTL Atlas: a powerful tool for trait dissection,
917 comparative genomics and crop improvement. *Theor Appl Genet*. doi:10.1007/s00122-
918 018-3212-5.

919 103. Gillis J, Mistry M, Pavlidis P (2010) Gene function analysis in complex data sets using
920 ErmineJ. *Nat Protoc* 5(6):1148–1159.

921 104. Brewer PB, et al. (2016) LATERAL BRANCHING OXIDOREDUCTASE acts in the final
922 stages of strigolactone biosynthesis in Arabidopsis. *Proc Natl Acad Sci USA*
923 113(22):6301–6306.

105. Liu W, et al. (2011) Strigolactone biosynthesis in *Medicago truncatula* and rice requires the symbiotic GRAS-type transcription factors NSP1 and NSP2. *Plant Cell* 23(10):3853–3865.

106. Szpiech ZA, Hernandez RD (2014) selscan: an efficient multithreaded program to perform EHH-based scans for positive selection. *Mol Biol Evol* 31(10):2824–2827.

SUPPLEMENTAL DATA FILES:

Supplemental Data File S1: Sorghum accessions from the GBS dataset with predicted *LGS1* loss-of-function alleles. Botanical race is coded as 'NA' if accession was not found in master list of accession annotations. Accessions with missing data at SNP S5_69985710 tagging the frameshift are not included in this list

Supplemental Data File S2: Differentially expressed genes between nutrient-stressed roots of *Striga*-susceptible sorghum line Shanqui Red and *Striga*-resistant line SRN39.

Supplemental Data File S3: *Striga hermonthica* occurrence records used for species distribution models presented in this study.

Supplemental Data File S4: Raster file of MaxEnt logistic output for all-occurrence *S. hermonthica* species distribution model.

Supplemental Data File S5: Raster file of MaxEnt logistic output for sorghum-only *S. hermonthica* species distribution model.

SUPPLEMENTAL MATERIAL & METHODS:

Collection of sorghum root exudates.
Accessions were grown individually in two-gallon pots with 70% potting mix (Premier pro-mix PGX) and 30% medium commercial grade sand in a greenhouse at 85°F during the day and 75°F at night with a 16-hour photoperiod. Pots were fertilized with 1x strength Miracle-Gro (Miracle-Gro® Water Soluble All Purpose Plant Food, The Scotts Company, LLC., Marysville, OH) once at fourteen days after planting. Forty-three days after planting, potting components were carefully washed from roots and whole plants were placed in separate flasks with a 1:5 ratio of root:DI water (v/v). Flasks were sealed

with parafilm to prevent evaporation and placed into darkness at room temperature. After 48 hours, root exudate from each plant was centrifuged at 9,000 rpm for 10 minutes before removing supernatant for germination assays.

Root RNA extraction and DNase treatment.

For RNA extraction, root tissues were ground in liquid nitrogen using mortar and pestle. Ground tissue powder was homogenized using an equal volume (W/V) of TRIzol™ reagent (Invitrogen, Cat#15596018) and 1 mL homogenate was used in RNA extraction. RNA extraction generally followed TRIzol™ Reagent user guide. In brief, 200 µL of Chloroform:Isoamyl alcohol 24:1(Sigma, C0549) was added to 1 mL homogenate and incubated for 10 min on rotator mixer at room temperature. The homogenate was centrifuged at 12000 RCF for 15 min at 4^{o}C. The clear upper aqueous phase was transferred to new 1.5 mL Eppendorf tubes and combined with an equal volume (V/V) of isopropanol to precipitate nucleic acid. Samples were mixed well by inverting the tubes several times and centrifuged as described above to obtain RNA pellet. The supernatant was discarded and the pellet washed with 75% alcohol. The pellet was air dried for 10 min at room temperature and suspended in 30 µL of 10 mM Tris-Cl (pH 8.0). RNA samples were left overnight in 4^{o}C refrigerator to dissolve the pellet. Further, RNA samples were treated with DNase I (Ambion^{TM}, AM2222) to remove contaminating DNA. In brief, 25 µL of RNA was incubated with 2 units of DNase I and 3 µL of 10X DNaseI buffer for 30 minutes at 37^{o}C using a water bath. The nucleic acid was re-precipitated, air dried and dissolved in 25 µL of 10 mM Tris-Cl (pH 8.0). The RNA was quantified using NanoDrop® ND-1000 Spectrophotometer and ~100 ng of RNA was analyzed by 1% gel electrophoresis to verify that the RNA was intact and free of genomic DNA contamination.

Library preparation and sequencing.

We used 3'-TagSeq approach (Meyer *et al.,* 2011) with several modifications to construct cDNA libraries. This method focuses on 3' end of transcripts enriched in a size range of 400-500 bp fragments. Briefly, 1 µg of total RNA from each samples were prepared in a volume of 10 µL and incubated with 8 µL of degradation buffer (0.5mM dNTP mix, 1 mM DTT, 1X first strand buffer, 1 µM 3ILL-30TV oligo-dT primer to aim 3' ends of cDNA) at 70^{o}C for 16 min to achieve desire range of RNA fragments (300-600 bp). The entire fragmented RNA was further used in first strand cDNA (FS cDNA) synthesis with RNA oligo primer (S-ILL-swMW) and SMARTScribe Reverse Transcriptase (Clonetech). Then, cDNA was amplified with 16 cycles using Titanium Taq Polymerase, 3ILL and 5ILL primers, and 10 µL of the FS cDNA as template. The amplified cDNA products were purified using NucleoFast PCR Clean-up kit (Machery-Nagel) and quantified using Qubit dsDNA High sensitivity Assay Kit (Invitrogen) on Qubit® 2.0 Fluorometer.

Further, 50 ng of purified cDNA from each sample was individually barcoded with four cycles of barcoding PCR. We used Illumina specific barcodes (ILL-BC) and multiplexed those using Illumina TruSeq universal adapters (TrusSeq_Un) for use on the Illumina platform. An equal volume of barcoded cDNA libraries was pooled together and purified using PureLink Quick Gel Extraction and PCR Purification Combo kit (Invitrogen). The purified cDNA library pool was separated on 1.5% agarose in 1X TBE buffer (pH 8.2) to excise the fragment in the 400-500 bp size range. The excised gel fragment was purified using a gel extraction kit as mentioned above. The resulting library pool was loaded into a single lane of an Illumina Hiseq-2500 analyzer at the Genomic Sequencing and Analysis Facility at the University of Texas at Austin. We recovered between 3 to 5 million raw single-end 100 bp reads per sample. All primers used in the library preparation are given below.

Bioinformatic analysis of TagSeq data.

Briefly, we excluded reads containing more than 20 bp with Phred quality scores <20, homopolymer runs longer than 30 bp, or at least one 12-mer match to Illumina adaptor sequences. Reads were trimmed to remove non-template bases introduced during library prep, identified based on occurrence of a 'GGG' motif within the first 10 bp. Reads were then mapped to the set of 34,211 primary transcripts from the *S. bicolor* v3.1 genome with SHRiMP v.2.2.3 (David *et al.* 2011) and we kept only unique alignments and those with more than 40 bp matching the reference.

Oligos used in library preparations

TruSeq_Un1: AAT GAT ACG GCG ACC ACC GAG ATC TAC ACA TCA CGA CAC TCT TTC CCT ACA CGA CGC TCT TCC GAT CT

TruSeq_Un2: AAT GAT ACG GCG ACC ACC GAG ATC TAC ACA CTT GAA CAC TCT TTC CCT ACA CGA CGC TCT TCC GAT CT

ILL-BC (8 six-mer barcodes, here shown as NNNNNN):
CAAGCAGAAGACGGCATACGAGATNNNNNNGTGACTGGAGTTCAGACGTGTGCTC TTCCGATC

S-Ill-swMW:
rArCrCrCrCrArUrGrGrGrGrCrUrArCrArCrGrArCrGrCrUrCrUrUrCrCrGrArUrCrUrNrNMW rGrGrG

3ILL-30TV: ACGTGTGCTCTTCCGATCTAATTTTTTTTTTTTTTTTTTTTTTTTTTTTV

5ILL: CTACACGACGCTCTTCCGATCT

References

David, M., Dzamba, M., Lister, E., Ilie, L., Brudno, M. (2011). SHRiMP2: Sensitive yet Practical Short Read Mapping. *Bioinformatics.* 27, 1011-1012.

Meyer, E., Aglyamova, G. & Matz, M. (2011). Profiling gene expression responses of coral larvae (Acropora millepora) to elevated temperature and settlement inducers using a novel RNA-Seq procedure. *Mol. Ecol.* 20, 3599–3616.

Supplemental Figures:

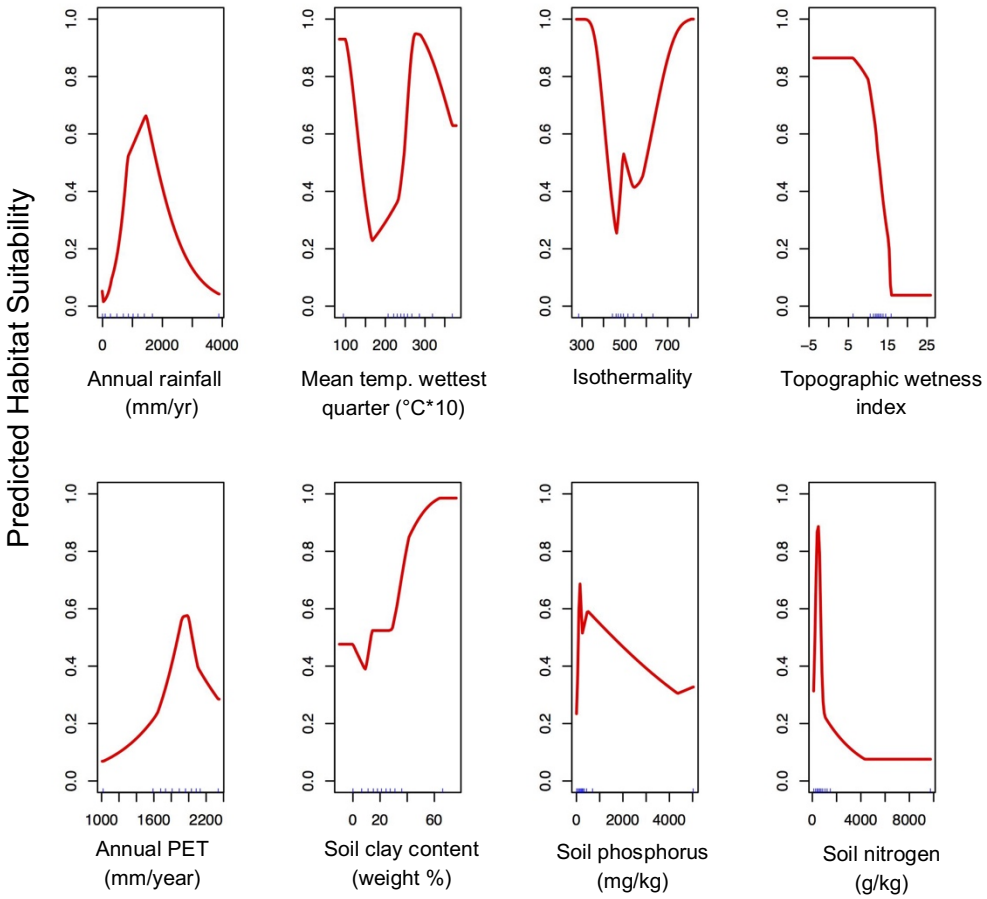

Supplemental Figure S1. Response curves for 8 environmental variables in all occurrence *S. hermonthica* distribution model. Curves represent the change in predicted habitat suitability (y-axis) for each variable with all other variables held at a constant value.

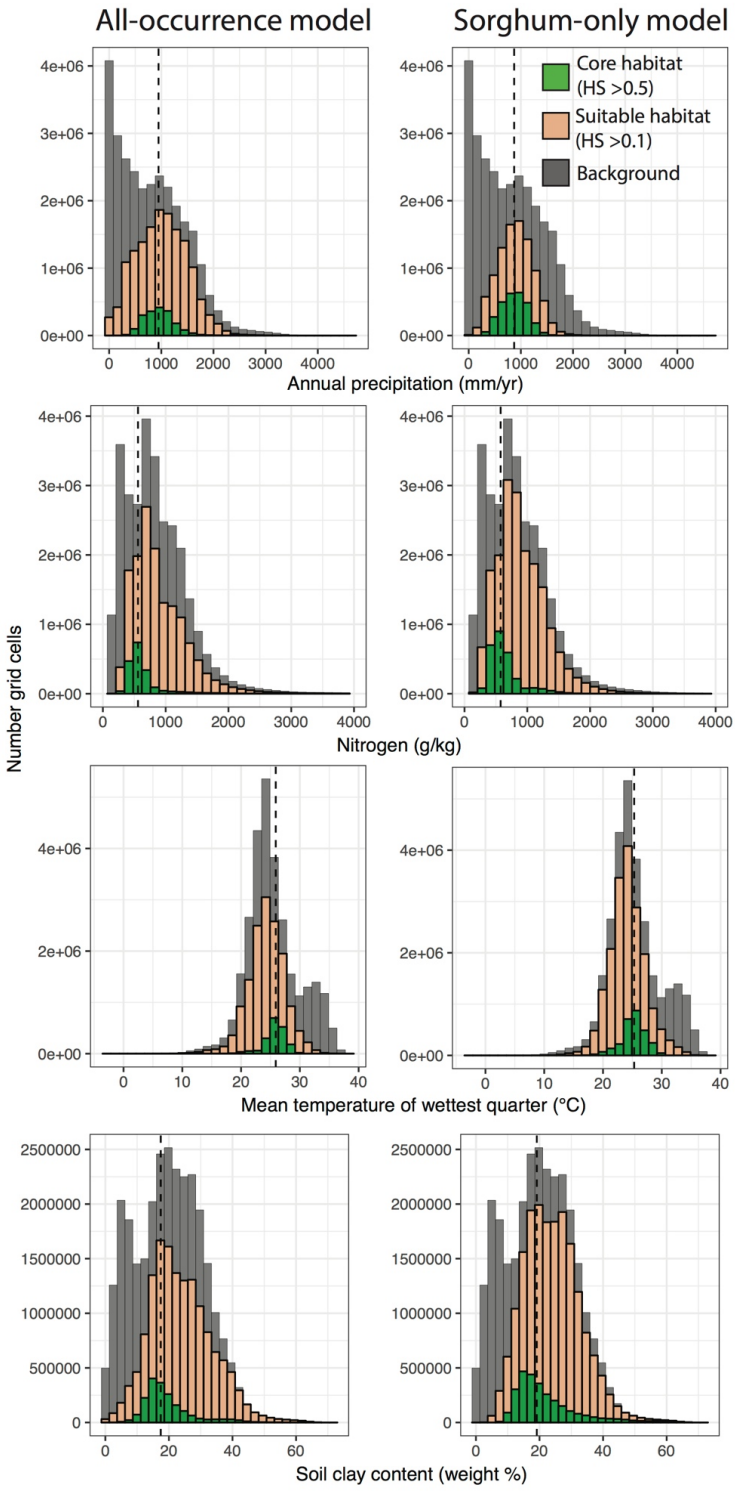

Supplemental Figure S2. Distribution of environmental values for four variables with permutation importance greater than 10% for the all-occurrence or sorghum-only *S. hermonthica* SDMs. Distributions are shown for all grids cells exceeding habitat suitability (HS) scores of 0.5 or 0.1, or for all grid cells in the background.

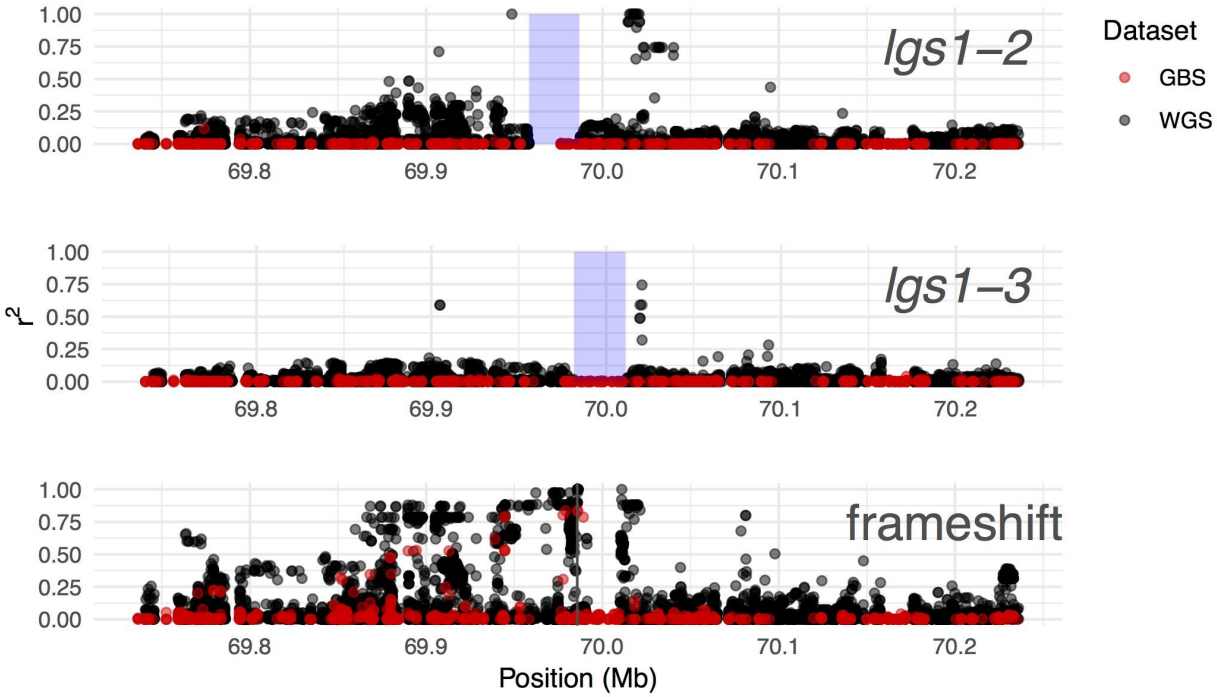

Supplemental Figure S3. Linkage disequilibrium with large deletion variants and the frameshift mutation at position 69,986,146 on *S. bicolor* Chromosome 5. Shaded boxes indicate positions of deletions (*lgs1-2*: 69,958,377-69,986,892*; lgs1-3*: 69,981,502-70,011,149) and vertical line indicates position of SNP tagging the frameshift mutation in the GBS dataset. For the WGS dataset, we excluded genotypes with depth of coverage less than 5x and SNPs with >70% missing data. Due to large amounts of missing data in the GBS dataset, r^2 was calculated based on imputed SNPs. An 18.8kb deletion beginning at position 69,991,579 also occurs in accessions with the frameshift, leading to missing data in this region for the non-imputed (WGS) dataset.

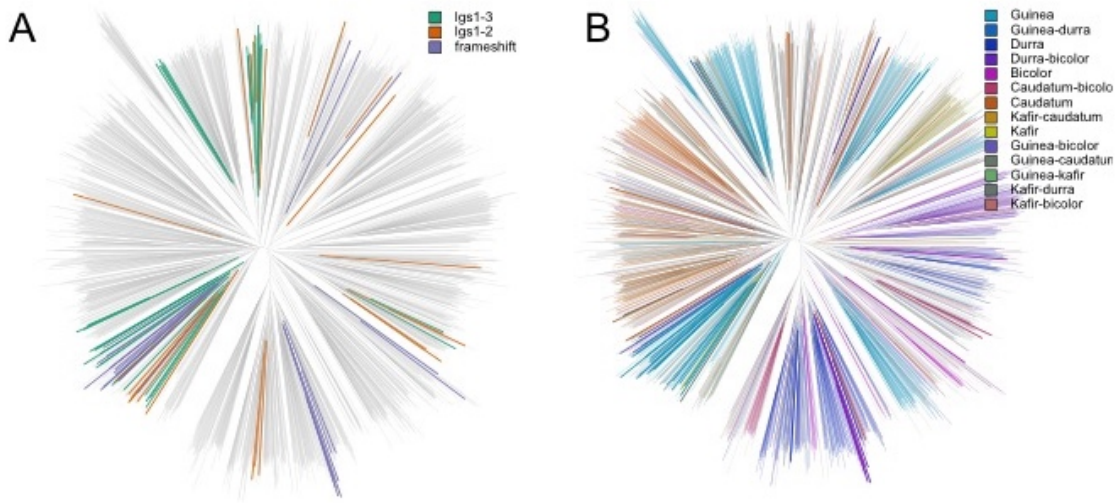

Supplemental Figure S4. Unrooted neighbor joining tree for *S. bicolor* chromosome 5 based on 2070 georeferenced individuals and 5434 SNPs with MAF >1%, after removing SNPs with >30% missing genotype calls. Branches are color-coded according to LGS1 deletion allele (A) or botanical race (B).

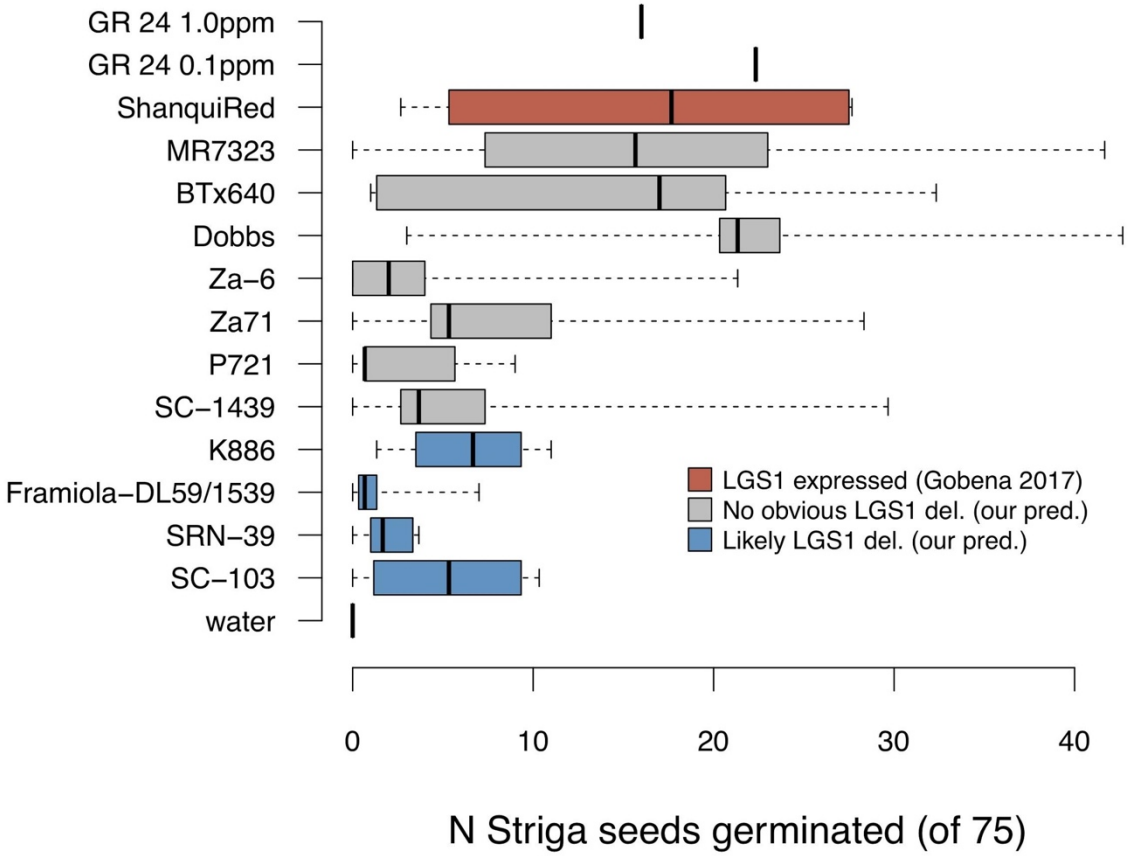

Supplemental Figure S5. Germination of *S. hermonthica* in response to root exudates isolated from 12 sorghum varieties. Boxes show interquartile range and median, whiskers show maximum and minimum. Predictions for LGS1 deletions are based on genotypes from the GBS dataset.

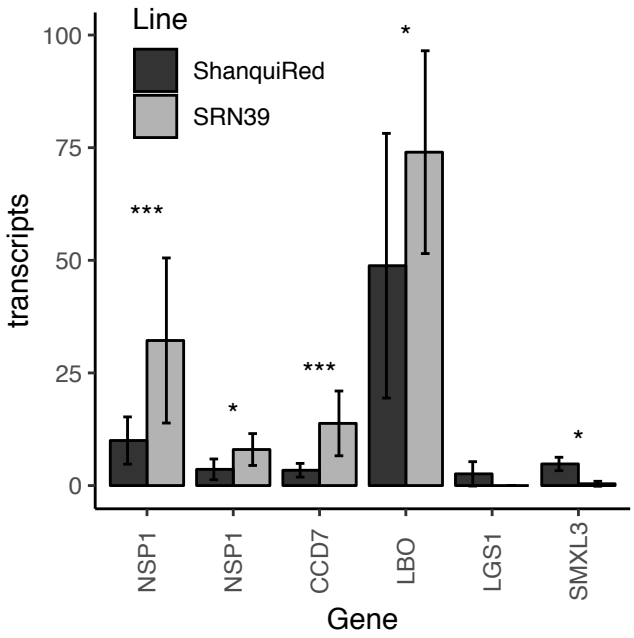

Supplemental Figure S6. Strigolactone biosynthesis and signaling pathway genes differentially regulated between nutrient-stressed roots of *LGS1*-deficient sorghum line SRN39 and *LGS1*-intact line Shanqui Red. Mean and standard deviation of read counts from 5 biological replicates per line are shown. Asterisks indicate significance following FDR correction. ***$p < 0.001$; **$p < 0.01$; *$p < 0.05$.

Table S1. Environmental predictors for species distribution models. Core ranges are given as the 10th and 90th percentiles for grid cell values within the study extent (18W to 62E; 37S to 38N) with habitat suitability score >0.5 (all-occurrence and sorghum-only models) or for all grid cells within the full study extent. Median values are shown in parentheses. Models showed good discrimination ability with AUC values of 0.86 (all-occurrence model) or 0.85 (sorghum-only model). Both models included linear, quadratic, hinge, and product feature classes with a regularization multiplier of 1 for the all-occurrence model or 4 for the sorghum-only model. PI: Permutation importance

Variable	Units	Source	PI, % (all-occurrence)	PI, % (sorghum-only)	Core range (all-occurrence	Core range (sorghum-only)	Core range (full extent)
Annual rainfall (Bio12)	mm/year	CHELSA	35.6	28.7	608-1307 (947)	543-1183 (871)	42-1665 (737)
Total nitrogen at 0-30 cm depth (NTO)	g/kg	AfSoilGrids250m	24.3	28.8	411-932 (559)	399-977 (575)	257-1449 (766)
Clay fraction at 5 cm depth (CLYPPT)	weight %	SoilGrids250m	4.6	24.0	12-29 (17)	13-36 (19)	5-34 (20)
Mean temperature of wettest quarter (Bio8)	°C	CHELSA	15.4	4.0	23.8-27.8 (25.9)	22.5-27.8 (25.3)	20.6-32.3 (24.7)
Isothermality (Bio3)	-	CHELSA	8.1	4.8	464-583 (485)	464-573 (486)	433-622 (491)
Topographic wetness index (topoWet)	-	ENVIREM	6.5	6.6	11.1-13.5 (12.5)	10.5-13.8 (12.5)	10.4-14.6 (12.6)
Potential evapotranspiration (annualPET)	mm/year	ENVIREM	4.0	2.9	1774-2044 (1937)	1789-2090 (1958)	1540-2126 (1821)
Total phosphorus at 0-30 cm depth	mg/kg	AfSoilGrids250m	1.6	0.2	117-426 (192)	119-465 (211)	63-653 (264)

1097 Table S2. *LGS1* loss-of-function mutations for African landraces in the WGS dataset

Accession	Origin	Race	SV type	SV size (bp)	Start	GT
PI221651	Nigeria	Guinea	Insertion	2	69986146	1/1
PI221651	Nigeria	Guinea	Deletion	315	69984268	1/1
PI329338	Ethiopia	Caudatum-bicolor	Insertion	2	69986146	1/1
PI562781	Mali	Guinea	Deletion	29647	69981502	1/1
PI562971	Nigeria	Other	Deletion	28515	69958377	1/1
PI562981	Nigeria	Other	Deletion	28515	69958377	1/1
PI562982	Nigeria	Guinea	Deletion	28515	69958377	1/1
PI562990	Nigeria	Other	Insertion	2	69986146	1/1
PI562990	Nigeria	Other	Deletion	315	69984268	1/1
PI562991	Nigeria	Other	Deletion	28515	69958377	1/1
PI562994	Nigeria	Other	Deletion	28515	69958377	1/1
PI562998	Nigeria	Other	Insertion	2	69986146	1/1
PI563002	Nigeria	Other	Insertion	2	69986146	1/1
PI563009	Nigeria	Guinea-caudatum	Deletion	29647	69981502	1/1
PI563020	Nigeria	Other	Deletion	29647	69981502	1/1
PI563021	Nigeria	Unknown	Insertion	2	69986146	1/1
PI563021	Nigeria	Unknown	Deletion	315	69984268	0/1
PI563022	Nigeria	Other	Insertion	2	69986146	1/1
PI563022	Nigeria	Other	Deletion	315	69984268	1/1
PI585406	Nigeria	Guinea	Insertion	2	69986146	1/1
PI585406	Nigeria	Guinea	Deletion	315	69984268	1/1
PI585448	Ghana	Guinea	Insertion	2	69986146	1/1
PI585448	Ghana	Guinea	Deletion	315	69984268	1/1
PI585448	Ghana	Guinea	Deletion	29647	69981502	0/1
PI585452	Ghana	Guinea	Insertion	2	69986146	0/1
PI585452	Ghana	Guinea	Deletion	315	69984268	0/1
PI585467	Ghana	Guinea	Insertion	2	69986146	1/1
PI585467	Ghana	Guinea	Deletion	315	69984268	1/1
PI585966	Togo	Guinea	Insertion	2	69986146	1/1
PI585966	Togo	Guinea	Deletion	315	69984268	1/1

1098

1099

Table S3: Sorghum genes related to strigolactone biosynthesis or signalling. The number of high impact variants with minor allele frequency (MAF) >5% in the WGS dataset are shown. Gene models with less than 5 SNPs were excluded from Tajima's D calculations. Expression for each gene model in root tissue of sorghum lines Shanqui Red and SRN39 are shown as the mean count for reads mapped, with asterisks indicating significant differences between lines. **adjusted p <0.001; *adjusted p <0.05

Homolog	Gene model	Function	Chr.	Pos.	Tajima's D	High impact variants (MAF >5%)	Expression
NSP1	Sobic.001G341400	GRAS-family transcription factor	1	62,864,836-62,867,833	NA	0	21.3**
NSP2	Sobic.001G428600	GRAS-family transcription factor	1	70,751,978-70,753,672	-0.51	0	3.0
D14	Sobic.001G465100	α/β-hydrolase	1	73,888,745-73,895,024	0.96	0	253
NSP1	Sobic.002G372100	GRAS-family transcription factor	2	73,049,658-73,053,841	-0.90	0	5.9*
CCD8	Sobic.002G380550	carlactone synthase	2	73,655,874-73,656,496	-0.84	1	0
MAX1	Sobic.003G269500	cytochrome P450	3	60,624,004-60,628,867	1.28	0	38.2
MAX1	Sobic.003G269600	cytochrome P450	3	60,633,944-60,636,136	0.92	1	73.4
CCD8	Sobic.003G293600	carlactone synthase	3	62,602,964-62,607,023	-0.23	0	24.0
LBO	Sobic.003G418000	oxidoreductase	3	72,382,455-72,384,461	3.80	0	60.6*
MAX1	Sobic.004G095500	cytochrome P450	4	8,304,449-8,307,025	2.39	0	0.4
SMXL5	Sobic.004G139900	Class I Clp ATPase	4	40,568,128-40,571,634	-0.07	0	1.5
SMXL3	Sobic.004	Class I Clp	4	51,922,148-	-0.19	2	1.9

	G168600	ATPase		51,925,516			
SMAX1	Sobic.004G325000	Class I Clp ATPase	4	66,043,348-66,044,531	0.54	0	57.0
SMXL7	Sobic.005G002400	Class I Clp ATPase	5	190,488-194,282	-0.64	0	3.9
CCD8	Sobic.005G002500	carlactone synthase	5	202,329-204,425	-1.41	4	0.26
SMXL3	Sobic.005G043000	Class I Clp ATPase	5	4,061,603-4,065,225[1]	0.74	3	24.3
CCD8	Sobic.005G105700	carlactone synthase	5	19,797,305-19,799,526	-2.15	0	1.4
D27	Sobic.005G168200	β-carotene isomerase	5	64,672,109-64,677,619	-0.88	0	3.0
LGS1	Sobic.005G213600	sulfotransferase	5	69,984,440-69,986,256	0.19	3	1.1
SMXL3	Sobic.006G074900	Class I Clp ATPase	6	43,746,994-43,751,171	-0.13	0	4.5
CCD7	Sobic.006G170300	β-carotene cleaving dioxygenase	6	52,713,305-52,716,037[2]	0.47	2	9.6**
D27	Sobic.007G016600	β-carotene isomerase	7	1,433,383-1,435,073	-1.13	0	0
SMAX1	Sobic.007G090900	Class I Clp ATPase	7	14,458,102-14,461,202	2.31	0	80.6
CCD8	Sobic.007G170300	carlactone synthase	7	60,503,029-60,506,362	-1.03	0	17.2
SMXL7	Sobic.008G002400	Class I Clp ATPase	8	219,391-225,260	0.26	0	245.2
SMXL3	Sobic.008G042800	Class I Clp ATPase	8	4,207,967-4,210,364	NA	0	2.2*
NSP2	Sobic.008G046700	GRAS-family transcription	8	4,591,222-4,596,201	-1.58	0	0.4

[1] Overlaps with $QTL05_1$ (Yohannes et al. 2015)
[2] Overlaps with QTL06 (Yohannes et al. 2015)

		factor					
D27	Sobic.009G030800	β-carotene isomerase	9	2,741,604-2,744,934	NA	0	13.9
MAX2	Sobic.010G043000	F-box protein	10	3,312,894-3,316,043	NA	0	222.1
MAX1	Sobic.010G170400	cytochrome P450	10	50,177,361-50,180,730	NA	0	33.7

D27: DWARF27; CCD7: CAROTENOID CLEAVING DIOXYGENASE 7; CCD8: CAROTENOID CLEAVING DIOXYGENASE 8; MAX1: MORE AXILLARY BRANCHES 1; NSP1: NODULATION SIGNALING PATHWAY 1; NSP2: NODULATION SIGNALING PATHWAY 2; LBO: LATERAL BRANCHING OXIDOREDUCTASE; LGS1: LOW GERMINATION STIMULANT 1; SMAX1: SUPPRESSOR OF MAX2-1; SMXL7: SMAX1-LIKE 7; SMXL5: SMAX1-LIKE 5; SMXL3: SMAX1-LIKE 3

Table S4. Sorghum SNPs showing significant genome-wide associations with *S. hermonthica* distribution (FDR correction at α=0.05). SNPs within 1kb of gene models are annotated and are ordered according to genomic location. AF: reference allele frequency; AdjP: P-value after FDR adjustment. For gene models with more than one SNP, the highest scoring position is shown. SNPs predicted to result in an amino acid change are shown in bold.

Chr	Position	AF	AdjP	Gene_model	Annotation
1	21828170[3]	0.292	0.046	Sobic.001G227800	Uncharacterized conserved protein, putative, expressed
1	50469815	0.035	0.037	NA	NA
1	54864458[4]	0.013	0.024	NA	NA
1	56800905	0.043	0.028	NA	NA
1	58808651	0.214	0.046	NA	NA
1	58837130	0.14	0.045	Sobic.001G304500	Os10g0551200 protein; GRAS domain family
1	64142276	0.052	0.024	NA	NA
1	64164495	0.054	0.004	Sobic.001G352600	Expressed protein
1	71929093	0.036	0.024	Sobic.001G441500	NA
2	12723171	0.028	0.035	NA	NA
2	21521798	0.275	0.013	Sobic.002G138400	Pectinesterase 14-related
2	68524689	0.018	0.049	Sobic.002G311400	Putative glucosyltransferase
3	1842885	0.011	0.045	NA	NA
3	2025341	0.012	0.002	Sobic.003G023500	Os06g0116300 protein; putative syntaxin
3	13445493	0.026	0.041	Sobic.003G139000	Os01g0290600 protein; putative L-cysteine desulfhydrase 2
3	51292869	0.012	0.023	NA	NA
3	56946323	0.055	0.043	Sobic.003G229700	glycerol-3-phosphate acyltransferase
3	59075308	0.018	0.008	Sobic.003G252200	HB1, ASXL, restriction endonuclease HTH domain (HARE-HTH)
3	62473154	0.077	0.002	NA	NA
3	62493603	0.093	0.028	Sobic.003G292500	ATP-dependent protease La (LON) domain-containing protein-like
3	62795897	0.012	0.002	Sobic.003G295900	Putative heat shock factor
3	67782723	0.012	0.008	Sobic.003G360200	WUSCHEL-related homeobox 9

[3] QTL from Haussman et al (2004) N13/E36-1
[4] QTL from Haussman et al (2004) N13/E36-1

3	70103330	0.055	0.017	Sobic.003G389700	Os01g0898800 protein
4	19466351	0.011	0.045	NA	NA
4	19724561	0.011	0.028	NA	NA
4	19735015	0.011	0.020	Sobic.004G132200	NA
4	20033536	0.014	0.040	NA	NA
4	20035072	0.012	0.027	NA	NA
4	20782140	0.012	0.012	NA	NA
4	23221234	0.041	0.012	NA	NA
4	60099891	0.012	0.002	Sobic.004G254500	Leafy cotyledon1
4	60767527	0.012	0.015	NA	NA
4	66105213	0.013	0.006	Sobic.004G325832	NA
4	66766354	0.03	0.040	NA	NA
5	1950501	0.087	0.045	NA	NA
5	1976589	0.086	0.013	Sobic.005G021400	NA
5	11089407	0.062	0.024	NA	NA
5	71122163	0.011	0.012	Sobic.005G224300	similar to O-methyltransferase
6	487441	0.086	0.040	Sobic.006G002900	similar to OSJNBa0094O15.15 protein; zinc/RING finger domain
6	15445897	0.011	0.046	NA	NA
6	42246344	0.129	0.028	NA	NA
6	43653802	0.022	0.018	Sobic.006G074300	similar to OSIGBa0092M08.2 protein; non-specific lipid transfer protein d6
6	51034850	0.028	0.033	NA	NA
6	51042152	0.079	0.050	Sobic.006G148800	Phenylalanine ammonia-lyase
6	52891272	0.087	0.004	NA	NA
6	59662162	0.012	0.042	Sobic.006G261700	similar to OSJNBb0004A17.4; Lactoylglutathione lyase
7	11575066	0.014	0.018	NA	NA
7	12044293	0.014	0.016	NA	NA
7	12094853	0.013	0.012	NA	NA
7	12891407	0.019	0.045	NA	NA
7	12895894	0.01	0.015	NA	NA
7	14193502	0.018	0.045	NA	NA
7	14220105	0.018	0.034	NA	NA
7	14279216	0.015	0.028	NA	NA
7	14459084[5]	0.014	0.007	Sobic.007G090900	ATP dependent CLP protease; SMAX1

[5] SL signaling (SMAX1 ortholog)

7	14942059	0.018	0.026	Sobic.007G091200	similar to H0117D06-OSIGBa0088B06.9 protein; Long-chain-alcohol O-fatty-acyltransferase
7	15219432	0.021	0.040	Sobic.007G091400	diacylglycerol kinase (ATP) (dgkA, DGK)
7	15254559	0.013	0.004	NA	NA
7	15325565	0.017	0.045	NA	NA
7	15359204	0.013	0.024	NA	NA
7	15532403	0.013	0.012	NA	NA
7	15534152	0.013	0.004	NA	NA
7	15554515	0.012	0.002	Sobic.007G092000	CCT/B-box zinc finger protein
7	15653673	0.019	0.046	Sobic.007G092200	aspartate carbamoyltransferase
7	15849206	0.014	0.027	NA	NA
7	15901805	0.017	0.026	NA	NA
7	15929687	0.019	0.018	Sobic.007G092600	Receptor-like kinase Xa21-binding protein 3-like
7	16293907	0.014	0.027	NA	NA
7	17082700	0.014	0.044	NA	NA
7	17092629	0.017	0.040	Sobic.007G093900	N-terminal acetyltransferase
7	17302379	0.019	0.045	Sobic.007G094600	Cytochrome P450 protein
7	17831891	0.019	0.040	Sobic.007G096200	Putative uncharacterized protein
7	17882047	0.018	0.028	NA	NA
7	17960172	0.018	0.018	Sobic.007G096800	Putative uncharacterized protein
7	18275486	0.012	0.018	NA	NA
7	18279010	0.013	0.015	NA	NA
7	18300164	0.012	0.024	NA	NA
7	18408217	0.012	0.015	NA	NA
7	19041599	0.011	0.037	Sobic.007G097400	sin-like protein conserved region containing protein
7	48195744	0.017	0.045	NA	NA
7	62605107	0.013	0.006	Sobic.007G193500	similar to Teosinte glume architecture 1
7	63109499	0.023	0.045	NA	NA
8	3177383	0.024	0.029	Sobic.008G034400	ATP-dependent RNA helicase, putative, expressed
8	13233629	0.016	0.018	NA	NA
8	60143889	0.012	0.026	Sobic.008G167300	Leucine-rich repeat-containing protein
8	61305329	0.014	0.043	Sobic.008G179600	similar to Expressed protein
9	1792519	0.011	0.017	Sobic.009G019900	NA

9	5744893	0.226	0.046	Sobic.009G056600	Putative uncharacterized protein
9	49976645	0.014	0.028	Sobic.009G142400	Putative gibberellin 20-oxidase
9	51474569	0.110	0.028	NA	NA
9	56421520	0.014	0.040	NA	NA
10	13677824	0.014	0.024	NA	NA
10	55681432	0.020	0.013	Sobic.010G213900	Receptor protein kinase PERK1-like
10	56006575	0.014	0.014	Sobic.010G216800	Putative uncharacterized protein
10	56761438[6]	0.026	0.018	NA	NA
10	59272319	0.016	0.028	Sobic.010G253700	NA

[6] QTL from Haussman et al (2004) IS9830/E36-1

1122 Table S5. Accessions from the Sorghum Association Panel used in germination study.

Accession	Name	Origin	Reported Resistance	*LGS1* allele
PI 656027	SRN39	-	Resistant	Deletion
PI 533752	SC103 (54.K.94)	-	Resistant	Deletion
PI 533972	Dobbs	Uganda	Resistant	Intact
PI 656025	Shanqui Red	China	Susceptible	Intact
PI 656055	P721	US	Susceptible	Intact*
PI 656051	MR7323	Niger	Unknown	Intact
PI 642791	BTx640	US	Unknown	Intact
PI 534088	Za6	Nigeria	Unknown	Intact
PI 534092	Za71	Nigeria	Unknown	Intact
PI 533976	Framiola DL59/1539	South Africa	Unknown	Deletion
PI 656040	K886	-	Unknown	Deletion
PI 656081	SC1439	-	Unknown	Intact*

1123 *No data in coding region, although SNP calls inconsistent with breakpoints for *lgs1-2* or
1124 *lgs1-3*.
1125